Deep sequencing reveals that early reprogramming of Arabidopsis root transcriptomes upon *Ralstonia solanacearum* infection

Cuizhu Zhao[1], Huijuan Wang[1], Yao Lu[1], Jinxue Hu[1], Ling Qu[2], Zheqing Li[1], Dongdong Wang[1], Yizhe He[1], Marc Valls[3,4], Núria S. Coll[4], Qin Chen[1*] and Haibin Lu[1*]

[1]State Key Laboratory of Crop Stress Biology for Arid Areas, College of Agronomy, Northwest A&F University, Yangling, Shaanxi, China. 712100

[2]National Wolfberry Engineering Research Center, Ningxia Academy of Agriculture and Forestry Sciences, Yinchuan, Ningxia.750002

[3]Genetics section, Universitat de Barcelona, 08028 Barcelona, Catalonia, Spain.

[4] Centre for Research in Agricultural Genomics (CRAG), CSIC-IRTA-UAB-UB, 08193 Barcelona, Catalonia, Spain.

[*] Corresponding author: chenpeter2289@nwsuaf.edu.cn and luhaibin011@hotmail.com Tel: +0086-18829010553

RunningTitle: Root Transcriptional Responses to *R. solanacearum*

Word count: 6988 words

Keywords: root defense, transcriptome profiling, *Ralstonia solanacearum,* plant hormones, bacterial wilt, RNA sequencing, root growth inhibition, lateral root formation, root hair formation.

SUMMARY

Bacterial wilt caused by the bacterial pathogen *Ralstonia solanacearum* is one of the most devastating crop diseases worldwide. The molecular mechanisms controlling the early stages of *R. solanacearum* colonization in the root remain unknown. In this study we established four stages in the early interaction of the pathogen with Arabidopsis roots and determined the transcriptional profiles of these stages of infection. A total 2698 genes were identified as differentially expressed genes during the initial 96h after infection, with the majority of changes in gene expression occurring after pathogen-triggered root hair development was observed. Further analysis of differentially-expressed genes indicated sequential activation of multiple hormone signaling cascades, including abscissic acid (ABA), auxin, jasmonic acid (JA), and ethylene (ET). Simultaneous impairment of ABA receptor genes increased plant sensitivity to *R. solanacearum*, but did not affect primary root growth inhibition, root hair and lateral root formation caused by *R. solanacearum*. This indicates that ABA signaling positively regulates root defense to *R. solanacearum*. Moreover, transcriptional changes of genes involved in primary root, lateral root and root hair formation exhibited high temporal dynamics upon infection. Taken together, our results suggest that successful infection of *R. solanacearum* on roots is a highly programmed process involving in hormone crosstalk.

INTRODUCTION

Ralstonia solanocearum, a soil-borne phytopathogen, causes devastating bacterial wilt disease on crops and leads to huge economical loss (Mansfield et al., 2012). The bacterium enters into the root epidermis through natural openings or wounds, crosses the cortex and endodermis and finally reaches the root xylem. In the xylem, *R. solanacearum* starts extensive colonization, spreading to the aerial part of the infected plant along the vascular system and finally kills the host by blocking water transport from root to shoot, which causes the wilting symptoms (Genin and Denny, 2012). Due to its wide host range, long persistence in soil and water and broad geographical distribution, *R. solanacearum* was ranked as the second most important bacterial plant pathogen (Mansfield et al., 2012).

The interaction between *R. solanacearum* and Arabidopsis has been successfully used for more than twenty years as a model to study plant defense (Deslandes et al., 1998). However, our knowledge about the molecular mechanisms used by Arabidopsis to defend against *R. solanacearum* is still limited. *RRS1-R* is the only *R. solana*cearum resistance gene cloned from Arabidopsis and encodes a Toll-IL-1 receptor-nucleotide binding site-leucine rich repeat (TIR-NB-LRR) resistance protein with a C-terminal WRKY DNA-binding motif (Deslandes et al., 2002). In the absence of PopP2, an effector from *R. solanacearum* GMI1000, RRS1-R forms heterodimer complex with RPS4, another NB-LRR protein, localizes in the nucleus and binds DNA through WRKY domain. When PopP2 is delivered into the host cell through the Type Three Secretion System (TTSS), it directly interacts with the RPS4/RRS1-R resistance complex and acetylates WRKY domain of RRS1-R through its acetyltransferase activity, blocking RPS4/RRS1-R DNA-binding activity and activating RPS4-mediated plant resistance (Le Roux et al., 2015; Sarris et al., 2015).

It is widely recognized that the phytohormones salicylic acid (SA), jasmonate (JA) and ethylene (ET) play a determinant role in plant defense to diverse

pathogenic insects, bacteria and fungi. However it is still not clear what is the precise role of these hormones in response to *R. solanacearum*. Arabidopsis mutants deficient in biosynthesis or signaling of SA, JA and ET have been used to investigate their sensitivity to *R. solanacearum*, which has led sometimes to contradictory results. For instance, while an increase or decrease of endogeneous SA levels did not alter plant sensitivity to *R. solancearum* (Hirsch et al., 2002), depletion SA in *wat1* mutant though overexpression of the bacterial SA hydroxylase gene *NahG* restored plant susceptibility to *R. solanacearum* (Denance et al., 2013). Mutation of EIN2, an important component in ET signal transduction, dramatically delayed bacterial wilt on Arabidopsis, which did not happen on *etr1-3*, *ein4-1* and *eni3-1*, other ET insensitive mutants (Hirsch et al., 2002). In addition, while, the *jar1-1* mutant -lacking the bioactive JA-Ile- shows the same sensitivity to *R. solanacearum* as wild type plants (Hirsch et al., 2002), loss of function of the JA receptor *COI1-1* enhances plant defense against to *R. solanacearum* (Hernandez-Blanco et al., 2007).

WRKY transcription factors, critical players in modulating plant resistance to phytopathogens, were also reported to function in plant defense to *R. solancearum*. WRKY27 mutation delays disease symptom development by modulating signaling between the phloem and the xylem (Mukhtar et al., 2008). Inactivation of WRKY53 also reduces wilt symptom caused by *R. solanacearum* (Hu et al., 2008).

In roots, the cell wall is the first physical layer of plant defense against pathogens. It is demonstrated that alteration of cell wall affects Arabidopsis defense to *R. solanacearum*. Cellulose synthases are required for secondary cell wall formation. Mutations of cellulose synthase genes (*CESA4*, *CESA7* and *CESA8*) confer enhanced resistance to *R. solanacearum* independently of SA, JA and ET but dependent on ABA (Hernandez-Blanco et al., 2007). Similarly, the *WALLS ARE THIN 1* (*WAT1*) gene is essential for secondary cell wall deposition. A mutation in *WAT1* leads to reduced cell elongation and

secondary wall thickness, but it also increases SA content and plant defense to vascular *R. solanacearum* (Denance et al., 2013). Furthermore, pectin homogalacturonan in the root cell wall was reported to be degraded after *R. solanacearum* infection (Digonnet et al., 2012).

Transcriptional profiles by RNA-seq have been employed to look for important events in plant defense against *R. solanacearum* in Arabidopsis. The *R. solanacearum* △*hrpB* mutant has a dysfunctional TTSS and loses the ability to invade host plants (Vasse et al., 2000). Plants infected with this mutant exhibit increased plant defense to subsequent virulent strain infection. Microarray analysis of transcriptional changes in aerial part of plants treated with GMI1000 △*hrpB* indicated that 26% of up-regulated genes were involved in the metabolism and signaling of ABA (Feng et al., 2012). In addition, comparison of transcriptional profiles from the aerial part of Arabidopsis Col-0 inoculated with GMI1000 at several time points identified many differentially expressed genes associated with ABA signaling pathways (Hu et al., 2008).

However, previous microarray studies focused on transcriptional changes in the aerial part of root-inoculated Arabidopsis with GMI1000. Since *R. solanacearum* is soil-borne and infects plant roots, direct investigation of transcriptional changes in infected plant roots at a series of time points will help disclosing the molecular mechanism of *R. solanacearum* infection. In this study, by means of high-resolution temporal analysis of host global transcriptional changes following pathogen infection, we identified several important events as the activation of the biosynthesis and signaling of different hormones, and further connected root structure changes to the transcriptional reprogramming following *R. solanacearum* infection. Our data provides a cornerstone to understand complicated regulation networks during the infection process of *R. solanacearum* in the root.

RESULTS

Characterization of Root Morphology Changes Following GMI1000 Infection

As previously reported, Arabidopsis seedlings roots exhibited primary root growth retardation, *de novo* root hair formation and cell death appearance around the root tip at 9 days after GMI1000 treatment (Lu et al., 2018). To refine the appearance time of the three root phenotypes, we investigated the root elongation of Arabidopsis seedling after infection with GMI1000 over time. Primary roots kept growing the first 24 hours post-inoculation (hpi). At 48 hpi, primary root growth was found to be inhibited by GMI1000 (Fig. 1A). Root hairs covered root tips around 24 hpi, while they did not appear in water-treated seedlings (Fig. 1B). Roots were immersed in Propidium Iodide (PI) -a DNA/RNA dye used to investigate cell integrity- and observed under confocal microscope. Cells in the root meristem area were alive at 24 hpi but already dead at 48 hpi (Fig. 1C). In addition, lateral roots emerged from primary roots treated with GMI1000 at 72 hpi and became apparent at 96 hpi. The number of these secondary roots on Arabidopsis root treated with GMI1000 was 4-5 fold higher than in water-treated plants (Fig. 1A and Fig. S1). According to these root structure changes over time, we divided the initial root infection by *R. solanacearum* into four phenotypic stages：No symptoms (NS) stage at 0-12 hpi, Root Hair (RH) emergence stage at 12-24 hpi , Primary root growth arrest and Cell death (PC) stage at 24-48 hpi and Lateral Root (LR) emergence stage at 48-72 hpi.

Time Series of Global Transcriptional Re-Programming in Roots Challenged with GMI1000

To understand the events taking place at different infection stages of *R. solanacearum*, we infected 7-day-old seedling roots *in vitro*, and collected root samples at 0 hpi, 6 hpi, 12 hpi, 24 hpi, 48 hpi and 96 hpi, extracted total RNA and sequenced the global transcripts of GMI1000-infected roots. Around 600

seedling roots were pooled into one sample. Three biological replicates per time point were directly subjected to RNA-IIlumina sequencing. An average of 33.9 million clean reads (range from 26.9-41.5 million) with Q30 > 90% were obtained per sample. More than 94 percent of clean reads were mapped to the Arabidopsis genome (Table S1). Aiming to disclose the molecular mechanism of early infection process of *R. solancearum*, we respectively compared *R. solancearum*-infected root transcriptomes at different infection time points with those obtained in water-treated roots after 96h and in GMI1000-treated roots at time 0h. The time series expression profiles identified a total of 2698 Arabidopsis genes as differentially expressed genes (DEGs) based on their significance in fold-change expression (padj<0.05) and at least a two-fold change in expression level (-1>log2>1) (Fig. 2 and Supplemental Data Set 1).

To analyze the overall patterns in gene expression during *R. solancearum* infection, the 2698 DEGs were clustered into 11 hierarchical clusters based on their expression patterns over time (Fig. 2). The list of genes in each cluster is presented in Supplemental data Set 2. These clusters group sets of genes that were sequentially induced upon pathogen challenge over time. The cluster VI genes started increasing at 12 hpi and peaked at HR stage (24 hpi), then slowly dropped back to basal level, which was the most quick response to *R. solanacearum* infection. The maximum level of cluster IV and V genes was at RH stage and PC stage (48 hpi), later 12h than that of cluster VI. Then cluster V quickly decreased. Comparing with relative long-lasting expression pattern of cluster V and IV, the highest expression level of cluster III genes was more concentrated in PC stage. The cluster I and II genes went up to maximum level at LR stage (72 hpi) and 96 hpi, which are the last induction clusters. The down-regulated genes also showed temporoally modulated expression pattern.The earliest repressed-gene clusters are cluster VIII and XI, which happened at RH stage. Interestingly, unlike cluster VIII maintaining lower expression, a few genes in cluster XI suffered a second induction at LR stage. The lowest expression level of cluster IX and cluster X occured at LR

stage.The expression of cluster VII were inhibited at LR stage and 96 hpi (Fig.2).

To check whether the co-expressing genes in the same cluster participated in similar biological processes, we investigated over-representation of Gene Ontology (GO) terms in these groups. The selected over-represented GO terms are shown at the right of each gene expression cluster in figure 2. Cell wall organization genes enriched in cluster VI unregulated before the appearance of root hairs (12 hpi) and reached their highest level at RH stage in response to the pathogen, reflecting cell wall remodeling has a specific role in the plant response to GMI1000 infection. A significant GO term in cluster V was lignin metabolic process. Cluster IV contained major GO terms: tryptophan metabolic process, auxin metabolic process and glucosinolate biosynthetic process, which share major components in their biosynthesis and peak at RH and PC stage. The GO term “response to auxin” was over-presented in cluster I, cluster II and cluster III and strongly induced during PC stage and LR stage (48-72 hpi), later 24 hour than GO term ”axuin metabolic process” in cluster VI (Fig. 2). Additionally GO terms such as “response to JA”, “response to abiotic stress”, “response to heat” and “response to hydrogen peroxide” were also overrepresented in clusters I, II and III. GO terms related with plant defense such as “response to chitin”, “response to bacterium”, “response to SA” and “defense response” were enriched in cluster VII, which were significantly suppressed during LR stage (72 hpi) . Interestingly, GO terms “cell to cell junction” and “cell wall organization“ also were enriched in Cluster VIII were significantly suppressed at PC and LR stage. Cluster X genes were significantly related with GO term “root hair cell differentiation”, which suppressed when lateral root emerging.

Biological processes that take place during *R. solanacearum* infection are likely to affect the outcome of the plant-pathogen interaction. Therefore we further investigated enriched GO terms in the DEGs at single time points irrespective of the previous clustering (Fig. S2). This analysis revealed that cell

wall organization-associated genes were enriched at NS and RH stages, suggesting that these genes probably contribute to loosening the cell wall and cell-to-cell junctions, which may help *R. solanacerum* crossing the cortex and endodermis at early infection stages. The term “tryptophan metabolic process” was overrepresented in up-regulated DEGs at RH stage, which may point at tryptophan as a likely substrate for auxin biosynthesis. “Response to biotic stimulus” was a GO term overrepresented in up-regulated DEGs at RH stage and PC stage. “Response to hormones” was overrepresented in genes specifically upregulated at PC and LR stages (48 hpi and 72 hpi, respectively), which may reflect the root structure changes that take place at the LR stage. The GO term “response to abiotic stimulus” was also highlighted in the upregulated DEGs at PC stage. The upregulated “Glucosinolate biosynthetic process” term spanned from LR stage to 96 hpi. JA is involved in root development and regulation of plant defense. The DEGs related to “Response to JA” term remarkably increased at 96 hpi. In down-regulated DEGs, the terms “transport”, “cell wall organization” and “root development terms” were over-represented at PC and LR stage. These sequentially overrepresented GO terms during early *R. solanacearum* infection indicate that infection is a programmed dynamic event from the very beginning of the plant-pathogen interaction.

Ethylene-, Jasmonate-, Auxin- and Abscissic acid-dependent signalling are altered following *R. solanacearum* Infection

The first and rate-limiting step in ethylene (ET) biosynthesis is the conversion of S-adenosyl Methionine to 1-aminocyclopropane-1-carboxylic acid (ACC) by ACC synthase (ACS). Five out of the nine *ACS* genes in the Arabidopsis genome (*ACS2*, *ACS6*, *ACS7*, *ACS8* and *ACS9*) were induced at PC stage. Interestingly, the expression of *ACS5* was inhibited at the same time (Fig. S3A). No ACC oxidase gene was identified in our RNA-seq data. However, its regulatror SHYG was induced at RH and PC stage (Rauf et al.,

2013) (Fig. S3A). Moreover, *ERF* transcriptional factors including *ORA59* and *ERF71* in response to ET were up-regulated or down-regulated following GMI1000 infection (Fig. S3A). These findings suggest that ET biosynthesis and signaling are involved in *R. solanacearum* infection.

The expression of several genes involved in jasmonic acid (JA) biosynthesis and degradation was also altered in our RNA-seq data. For example, *LOX1* and *LOX2,* encoding 13-lipoxygenase were induced at PC stage. LOXs are responsible for converting α-linolenic acid to 13-hydroxyperoxy-octadecatrienoic acid (13-HPOT) in plastids, which is the first step in the production of the JA precursor (Wasternack and Hause, 2013). However, Acyl-coenzyme A oxidase (ACX4) and 3-ketoacyl-CoA thiolase (KAT5), which catalize JA biosynthesis from this precursor (Li et al., 2005) were repressed after inoculation. Three of the four Arabidopsis jasmonate-induced oxygenases (JAOs), which inactivate JA through hydroxylation (Caarls et al., 2017), were highly expressed in our data. Similarly, a hydroxyjasmonate sulfotransferase (ST2A) that inactivates JA functions (Gidda et al., 2003) was highly induced at LR stage (Fig. S3B). Jasmonate ZIM domain Proteins (*JAZ1*, *JAI3*, *JAI5* and *JAZ10*), key negative regulators of JA signaling pathway, were strongly activated at LR stage and 96 hpi (Fig. S3B). In summary, the decrease in JA biosynthesis and increase in JA degradation and negative regulators suggests an inhibition of this pathway by *R. solanacearum* at late infection stages.

The components in auxin metabolism, auxin signaling and auxin transport were up-regulated from NS stage to LR stage (Fig. 3). *TRP4*, *TRP5*, *TRP1*, *TRP3* and *TSB2* encode five key components in the transformation of chorismate to the auxin precursor tryptophan (Zhao, 2010). All of them were up-regulated at RH stage (Fig 3A and Fig 3B). Members of two of the four tryptophan-dependent auxin synthesis pathways described in Arabidopsis (Zhao, 2010; Rosquete et al., 2012) were up-regulated at RH stage (genes *CYP79B2*, *CYP79B3*, *NIT1*, *NIT3* and *YUC9*) (Fig. 3A and Fig. 3B). In addition,

the expression of *DAO1* and *DAO2* -encoding genes that oxidate IAA to oxIAA and GH3 family genes, which conjugate amino acids to IAA (Rosquete et al., 2012) were all induced at RH and PC stages (Fig. 3A and Fig. 3B). Accumulation of auxin-responsive transcripts such *SAURs* and *Aux/IAAs* was observed at PC stage (Woodward and Bartel, 2005), which is 24 hours later than the peak auxin synthesis genes (Fig. 3B and Fig. S4). The expression of auxin response factors such as *Auxin Response Factor 4* (*ARF4*) increased during infection (Fig. 3C), as well as the expression of auxin efflux transporters (*PINs* and *ABCB4*) (Rosquete et al., 2012), which increased at PC and LR stages (Fig. 3D). Moreover, a few regulators of stability of auxin tranporters (*PATL2*, *RAM2*, *PBP1*, *PILS7*, *SMXL8* and *PID*) were also differentially expressed in our data.

Our RNA-seq data also identified a group of genes that were associated with abscissic acid (ABA) metabolism and signaling (Fig. 4A). The expression of *CYP707A,* which oxidizes and inactivates ABA (Saito et al., 2004), was induced at all time points after 24 hpi. Expression of the ABA receptor *PYL5* was inhibited after infection (Fig. 4A). And the *ABI2*, *HAB1* and PP2C5 genes, encoding protein phosphatases that suppress ABA signalling through dephosphorylation of SNRK2 proteins (Umezawa et al., 2009), were both up-regulated at PC stage. Expression of *OST1*, essential for ABA signaling (Fujii et al., 2009), showed a peak at PC stage, and then quickly decreased at LR stage. On the contrary, other *SNRK* family genes were inhibited at PC and LR stage (Fig. 4A). Finally, expression of the ABA-dependent transcription factor *ABF2* (Fujita et al., 2005) peaked at RH stage, 24 hours earlier than *OST1* (Fig. 4A).

ABA signaling is involved in plant resistance to *R. solanacearum*

Next, we investigated whether the alteration of ABA biosynthesis and signalling caused upon *R. solanacearum* infection had an impact on plant responses to this pathogen. To this end, we took advantage of available

Arabidopsis mutants: the quintuple *pyl1/pyl2/pyl4/pyl5/pyl8* (12458) and the sextuple *pyr1/pyl1/pyl2/pyl4/pyl5/pyl8* (112458) mutants, which are devoid of multiple ABA receptors and show reduced vegetative growth and seed production (Gonzalez-Guzman et al., 2012). We grew the Col-0 accession and ABA receptor mutants and tested their sensitivities to *R. solanacearum* infection. Both mutant lines showed increased wilting symptoms at 15 days post-inoculation compared with their wild type counterpart (Fig. 4B). This was translated into a significantly higher plant mortality rates in the mutants than in wild type plants (Fig. 4C). These results indicate a role of ABA signaling in plant resistance to *R. solanacearum*. We further tested if ABA signaling could affect the previously-described root morphology changes induced by the bacterium. The sextuple mutant exhibited root morphogenetic responses identical to wild type plants (Fig. 5), suggesting that ABA signaling is not required for *R. solanacearum*-induced root structural changes.

Regulation of Plant Defense Response genes in *R. solanacerum*-infected Roots

Among the 2698 genes differentially-expressed after *R. solanacearum* infection 109 have been previously involved in plant defense (Fig. S5 and Supplemental Data Set 3). RLK3, RD19 and WRKY27 regulate plant defense to *R. solanacearum*. RLK3 encoding a cysteine-rich repeat receptor like kinase was induced in the Arabidopsis ecotype Niederzenz (Nd-1) infected with *R. solanacearum* GMI1000 (Czernic et al., 1999). RLK3 was strongly induced at 12 hpi and reached a peak at PC stage in infected plants (Fig. S5). Surprisingly, RD19, a cysteine protease required for RRS1-R-mediated resistance to *R. solanacearum* (Bernoux et al., 2008) was strongly inhibited upon infection (Fig. S5). Similarly, WRKY27, which was shown to promote disease symptom development (Bernoux et al., 2008), was repressed upon infection (Fig. S5). The negative regulators of pathogen-associated molecular patterns (PAMP)-triggered immunity (PTI) PUB22 and PUB23 (Trujillo et al., 2008),

were differentially expressed with PUB22 downgoing and a earlier induction peak on PUB23. *LYK4* participating in sensing chitin was induced at 12h after infection and the expression of other PTI regulators (*PEP1*, *PUB23* and *MPK11*) was strongly induced at RH and LR stages. Interestingly, these genes were inhibited at LR stage (Fig. S5). Finally, 6 WRKY, 2 ERF and 2 ANAC transcription factors, key modulators of plant immunity, were also identified as DEGs in our experiments (Supplemental Data Set 3).

Transcriptional regulation of Programmed Plant Cell Death genes in *R. solanacearum*-infected roots

Programmed cell death (PCD) in root tip cells was initiated around 24 hpi and completed around 48 hpi after infection (Fig. 1C). In line with cell death appearance in root meristem zone, many regulators of plant cell death (PCD) were differentially expressed (Fig. 6). For instance, expression of two negative regulators of cell death -*MC2* and *SYP122*- (Zhang et al., 2008) (Coll et al., 2010) were strongly inhibited by *R. solanacearum* from RH stage on (Fig. 6A). Consistent with down-regulation of *SYP122*, the expression of mono-oxygenase1 (FMO1), required for SYP22-dependent lesion formation reached a peak at 24 hours after infection (Fig. 6A). Auto-inhibited Ca^{2+}-ATPase 4 (ACA4), also involved in regulation of PCD (Boursiac et al., 2010) was repressed at 24-48 hpi (Fig. 6A). In addition, we also noticed plant senescence genes associated with PCD differentially expressed (Fig. 6B). *Oresara1* (*ORE1*), a transcription factor regulating ET-mediated age-induced cell death, and WRKY57, a negative regulator of JA-induced leaf senescence (Jiang et al., 2014) were both strongly induced at RH stage, the latter starting induction at 12 hpi and decreasing at PC stage (Fig. 6B).

Root Architecture Responses to *R. solanacearum* Infection

Root hair formation was induced at RH stage at the root tip (Fig. 1B). We thus scrutinized our transcriptomes for differentially-expressed genes

described in the literature to play a role in this process. We found the root hair initiation zinc finger protein 5 (ZFP5) (An et al., 2012) and the *Oxidative signal-inducible 1* (*OXI1*) kinase required for normal root hair development (Rentel et al., 2004) were induced at 6hpi, peaking at RH stage and returning to basal levels at LR stage (Fig. 7A). The *ERU*, *EXP7* and *LRX1* genes, involved in root hair elongation (Baumberger et al., 2001; Lin et al., 2011; Schoenaers et al., 2018), were also quickly turned on at NS stage (6-12 hpi) and inactivated at PC stage (Fig. 7A). According to these data, root hairs should appear on root tips just after 12 hpi. We thus analysed in further detail root hair appearance by observing infected root tips at 6, 12, 18 and 24 hpi. Appearance of root hairs around the root tip was observed at around 18 hours after infection (Fig. 7B), which correlates to the changes in root hair gene expression patterns.

Another dramatic response to *R. solanacearum* infection is root growth inhibition. In our transcriptome data, many regulators involved in primary root growth were identified (Fig. 8). The expression of several negative regulators of root growth increased after infection, reaching the highest levels at PC stage. These included the *CLV3/ESR-related peptide 20* (*CLE20*) (Meng and Feldman, 2010), the methyltransferase PXMT1 (Chung et al., 2016) , the triterpene synthesis genes *THAH1*, *THAD1* and *THAS1* (Field and Osbourn, 2008), the LRP1 gene -involved in root growth retardation induced by phosphate deficiency (Svistoonoff et al., 2007) and *EFR,* whose gain-of-function mutant showed shorter primary roots in rice (Xiao et al., 2016). On the contrary, positive root growth regulators were repressed at PC stage. Amongst them are GA3ox catalyzing the final step in gibberellic acid (GA) biosynthesis (Mitchum et al., 2006) and *CLE6,* whose overexpression in a *ga3ox* mutant partially restored primary root growth (Bidadi et al., 2014). Therefore, coordinated expression of positive and negative regulators may control root growth inhibition induced by *R. solanacearum*.

The last morphogenetic change observed in infected roots was enhanced

appearance of secondary roots at 72 hpi. The transcript levels of the lateral root formation repressors CLE1, CLE3 and GLIP2 (Lee et al., 2009; Araya et al., 2014) were significantly decreased during LR stage. In addition, the positive secondary root regulators *GATA23*, were induced at 24 hpi and repressed from 48 to 96 hpi (Fig. 8). Interestingly, the action of *GATA23* is auxin-mediated (Xie et al., 2000; Lally et al., 2001; De Rybel et al., 2010; Lee and Kim, 2013), which suggests that auxin may be controlling this root response to *R. solanacearum*.

DISCUSSION

R. solanacearum causes genome-wide transcriptional reprogramming in Arabidopsis

Transcriptional reprogramming in aboveground tissue following soil-drenched *R. solanacearum* has been previously reported in Arabidopsis (Hu et al., 2008; Feng et al., 2012). Leaf transcriptome analysis from susceptible plants showed that 40% of the up-regulated genes were involved in ABA biosynthesis and signaling (Hu et al., 2008), which is line with our root transcriptome results. Similarly Feng and colleagues found that 26% of the upregulated genes in the leaf transcriptome pretreated with nonpathogenic *Ralstonia* strain were also involved in ABA biosynthesis and signaling. These indicate ABA signaling is triggered by pathogenic and nonpathogenic invasion and may function in root defense agnist *R. solanacearum*. Very few SA-associated genes were found in our root transcriptome, which also happened in the leaf transcrptome (Hu et al., 2008). This corroborates the notion that SA does not have a key role in plant defense responses against many root pathogenic bacteria. Moreover, several genes involved in auxin signaling were down-regulated in the leaf transcriptome (Hu et al., 2008). In contrast，the auxin biosynthesis, signaling and transport pathways were significantly induced in the root transcriptome reported here. This discrepancy in the results could be partly caused by the different tissues used in the

experiment (leaf vs. root) and different inoculation methods employed (soil drench vs. *in vitro* infection).

R. solanacearum manipulates different plant hormonal pathways

Plant hormones are well-known to synergistically or antagonistically affect each other's output, leading to plant resistance or susceptibility to various pathogens (Berens et al., 2017). Therefore，phytopathogens have acquired the abilities to hijack plant hormones to promote their proliferation in the host (Ma and Ma, 2016). Ethlyene and Jasmonic acid signals have been shown to be the main target of many virulence factors produced by biotrophic and hemibiotrophic phytopathogen, due to their negative role in plant immunity against biotrophic pathogens via SA antagonism (Kloek et al., 2001; Berrocal-Lobo et al., 2002). Ethlyene is produced by many plant pathogens including the bacterial pathogen *Pseudomonas syringae* and *R. solanacearum* (Weingart and Volksch, 1997; Valls et al., 2006). Disruption of ET production affects the virulence of *P. syringae* on soybean and bean (Weingart et al., 2001). In *R. solanacearum,* mutation of ethylene-forming enzyme (*RsEFE*) did not affect its proliferation on plant host (Valls et al., 2006). However plants defective in ethylene signaling (*ein2* mutants), show delayed wilt symptom (Hirsch et al., 2002). Our transcriptome data shows that *R. solanacearum* highly induces expression of *ACS* genes in the roots, which could indicate that besides directly producing ET, *R. solanacearum* employ another unknown stratedy to activate endogenous ET.

The *P. syringae* virulence factors Coronatine, HopZ1a, HopX1 and AvrB, virulence factors, activate JA signaling by promoting degradation of JAZ proteins, key negative regulators in JA signaling (Melotto et al., 2006; Jiang et al., 2013; Gimenez-Ibanez et al., 2014; Zhou et al., 2015). Activation of JA signaling leads to entry of phytopathgoen into apoplast by reopening closed stomata and attenuate SA-dependent plant defense (Melotto et al., 2006; Zhou et al., 2015). Hernandez-Blanco reported mutation in JA-Ile receptor gene,

Coronatine- insentistive 1 (*COI1*), conferred plant resistance to *R. solanacearum* (Hernandez-Blanco et al., 2007). Our data showed JA biosynthesis and degradation genes (*LOX1, LOX4* and *KAT5*) were differentially-expressed at earlier RH stage and *JAZs* were mainly induced at LR stage and 96 hpi, suggesting that JA signaing pathway was activated and then qucikly inhibited during *R. solanacearum* infection. However, the *jai3-1*, *jar1-1*, and *dde2* mutants with disabled JA biosynthesis or signaling showed similar root architectures as wild type plants in response to this pathogen (Lu et al., 2018). This indicates that JA may be involved in plant defense , but not in the root morphogenesis changes caused by *R. solanacearum*.

Auxin signaling and transport has been reported to be manupilated by phytopathogens to suppress activation of SA-dependent defense. The *P. syringae* effector AvrRpt2 activates auxin biosynthesis and induces expression of auxin-response genes by promoting degradation of the key negative regulators of auxin signaling AUX/IAAs. The effector HopM1 also from *P. syringae* and PSE1 from *Phytophthora parasitica* disrupt auxin transport by affecting expression or localization of different PIN auxin transporters, which promotes pathogen infection by antagonizing SA signaling (Nomura et al., 2006; Chen et al., 2007; Cui et al., 2013; Evangelisti et al., 2013; Tanaka et al., 2013). Many plant pathogens, including *R. solanacearum*, produce auxin-like molecules, which may alter auxin homestasis and affect auxin signaling in the host plants (Manulis et al., 1994; Glickmann et al., 1998; Valls et al., 2006; Robert-Seilaniantz et al., 2007). Interestingly, we oberserved that auxin biosynthesis genes were activated at the RH stage by *R. solanacearum* . Auxin signaling and transport were also upregulated at PC and LR stage. In line with our data, The expression of *DR5*, a marker gene of auxin signaling pathway, was strongly induced in root vascular after *R. solanacearum* GMI1000 infection (Lu et al., 2018). Moreover, the *dgl1-1* tomato mutant with disordered auxin transport was found to be highly resistant to *R. solanacearum* (French et al., 2018). Together, these data strongly supports the notion that auxin

signaling plays a negative role in root defense against *R. solanacerum*. A deeper understanding of the role of auxin signaling in plant susceptibility to *R. solanacearum* awaits further investigation.

ABA also plays an important role in attenuating plant defense, possibly by inhibiting SA signaling (Cao et al., 2011). Increase of ABA levels in infected plants will enhance plant susceptibility to the bacterial pathogen *P. syringae,* the fungus *Magnaporthe grisea* and the nematode *Hirshcmaniella oryzae* (de Torres-Zabala et al., 2007; Jiang et al., 2010; Nahar et al., 2012). In turn, various pathogenic fungi have been shown to produce ABA (Ma and Ma, 2016) and the effectors AvrPtoB and HopAM1 produced by *P. syringae* enhance plant susceptibility to the bacterial infection by promoting ABA biosynthesis or affecting ABA singaling (de Torres-Zabala et al., 2007; Goel et al., 2008). ABA also can positively regulate plant denfense to *P. syringae*. For example, ABA induces stomata closure and locks pathogen outside of host upon encountering pathogen, protecting plant from pathogen infection (Melotto et al., 2006). A large number of ABA-responsive genes were up-regulated in plants infected with the non-virulent *R. solanacerum* mutant *ΔhrpB* and in CESA4/CESA7/CESA8-mediated resistance to *R. solanacearum* (Hernandez-Blanco et al., 2007; Feng et al., 2012). *abi1-1* and *abi2-1*, two ABA-insensitive mutants, exhibited more sensitivity to *R. solanacearum* and disabled *Δhrp*B–triggered and CESA4/CESA7/CESA8- mediated plant resistance (Hu et al., 2008). Here we show that ABA signaling in root is turned on at PC stage, much earlier than activation of ABA signaling in leaf. Further genetic analysis demonstrated that simultaneous disruption of ABA receptors (12458 and 112458) dramatically enhanced susceptibility towards *R. solanacerum*. Consistent with this result, most components of the ABA receptor, *PYR1*, *PYL1*, *PYL2*, *PYL4*, and *PYL8,* express in the stele of root (Gonzalez-Guzman et al., 2012; Antoni et al., 2013). Interestingly, although both ABA receptor mutants are insensitive to ABA-mediated root growth inhibition (Antoni et al., 2013), they are still sensitive to root hair formation, root

growth inhibition, and lateral root formation caused by *R. solanacearum*. This indicates that ABA signaling is not essential for *R. solanacearum*-triggered root architechture changes. Together, our data suggests that ABA has a positive effect on plant defense against *R. solanacerum*. However, the precise mechanism by which ABA promotes defense to this bacteria still needs to be further elucidated

Together, all these data indicates that the interplay between R. solanacearum and Arabidopsis is mediated by a complex interplay of hormones. In particular, aa synergistic effect among JA, ET, SA, ABA, and auxin seem to determine the level of defense to *R. solanacearum* in the plant in spatiotemporal way. Our data provides new insight into the signaling network that occurs in the root host in response to a root pathogen.

***R. solanaceaum* infection triggers specific defense responses in the root**

PTI and Effector-triggered immunity (ETI) are the two layers of defense that plant pose to phytopathogens (Jones and Dangl, 2006). In our RNA-seq data, we identified several components of both defense branches, which is consistent with the reports that PAMPs elicits transcriptional changes and callose deposition in Arabidopsis root and the effector RBP1 from root nematode *Globodera pallida* triggers Gpa2-dependent resistance and cell death (Sacco et al., 2009; Millet et al., 2010). LYK4, PUB22, PUB23 and, PEP1 and MPK11, components of PTI signaling are quickly induced upon infection. Interestingly, all of these PTI-related genes were inhibited at LR stage, suggesting that *R. solanacearum* infection represses PTI in the root. In addition, we also found around 19 NBS-LRR resistance genes in DEGs including ZAR1. ZAR1 detects the acetylated hopz-ETI-deficient 1 (ZED1) by the *P. syringae* effector HopZ1a and triggers ETI (Lewis et al., 2010; Lewis et al., 2013). This suggests that this NB-LRR might be involved in *R. solanacearum* effector recognition.

Accompanying with ETI, hypersensitive response (HR), a local cell death

at the attempted entry site of pathogens, often happens. Cell death was observed on root tips at PC stage after *R. solanacearum* infection. Interestingly, the occurrence of *R. solanacearum*-mediated cell death at the root tip is dependent on the presence of a functional type three secretion system (Lu et al., 2018). This could indicate that this cell death occurs via effector recognition and thus ETI would be occurring at *R. solanacearum* infecting roots. HR in leaf is thought to directly kill invaders and/or to interfere biotrophic pathogen with acquisition of nutrients (Heath, 2000). But we showed cell death in root seems not to affect the virulence of GMI1000 on Arabidopsis and we know GMI1000 is a compatible strain on Arabidopsis. Necrotrophic pathogen triggers cell death in order to obtain more nutrients that helps them accomplishing their life cycle (Glazebrook, 2005). Whether *R. solanacearum* would follow a similar strategy with the root tip or it is simply a consequence of infection needs to be answered.

Root morphgenesis changes triggered by *R. solanacearum* infection are accompanied by deep transcriptional reprogramming of genes involved in root architecture

The root is embedded in the soil and its architecture determines the efficiency for nutrient uptake and aboveground growth. Root architecture is often shaped by biotic stress and abiotic stress such as interaction with mutualist microbes and elements deficiency (Le Fevre et al., 2015). Several *R. solanacearum* strains cause root morphological changes (Lu et al., 2018), reminiscent of root morphological changes triggered by plant growth promoting bacteria/rizobacteria or fungi (PGPB/PGPR and PGPF) (Verbon and Liberman, 2016). These beneficial microbes affect cell division at the root meristem region and cell differentiation at sites of lateral root formation through manipulating endogenous hormone levels, hormone signaling such as auxin signaling and transports and metabolic processes, resulting in root structure changes (Verbon and Liberman, 2016). Our transcriptiomic analysis indicated

that auxin synthesis, signaling and transport in root are all activated by *R. solanacearum* colonization. The auxin insensitive single mutant *tir1* and double mutant *tir1/afb2* were unable to form root hair in response to *R. solanacearum* infection (Lu et al., 2018). In consonance with this, IAA28 controlling the specification and identity of lateral root founder cells were upregualted in our data (De Rybel et al., 2010). This suggests that auxin signaling in relation to lateral formation might be activated in response to *R. solanacerum*. However, activation of auxin signaling enhances plant sensitivity to *P. syringae*, *Xanthomonas oryzae*, and *Magnaporthe oryzae* (Kazan and Lyons, 2014), whilst destruction of polar auxin transport in tomato tremendously elevated plant resistance towards *R. solanacearum* infection. This poses the question of whether the observed *R. solanacearum*-triggered architecture changes are side effects of elevated auxin levels caused by *R. solanacearum* to accomplish successful colonization or not. In addition, it is still not clear why *R. solanacearum* and PGPRs induce similar root architectures but exert two opposite influences on plant survival and what benefits does *R. solanacearum* obtain (if any) from altering root structure.

MATERIALS AND METHODS

Plants Materials

In this study, *Arabidopsis thaliana* Col-0 and the ABA receptor mutants *12458* and *112458* were sown in soil and grown in the chamber at 23 ºC, short day conditions(8h light, light intensity 12000 lux) and 70% humidity. For Arabidopsis seedling growth, Col-0 seeds were sterilized with 30% bleach and 0.02% TritonX-100, then sown on Murashige Skoog without sucrose (MS-) plate and grown with the plates set vertically at 25 ºC and long day conditions (16h light, light intensity 9000 lux for 6-7 days).

R. solanacearum **Infection**.

The strain *R. solanacearum* GMI1000 was used to infection in this study. For soil drench infection assay, 5-week old plants were watered with a suspension

of $1x10^8$ colony forming units (cfu). One hour later, roots of the infected plants were wounded three times with a blade, then grown into the chamber at 25 ºC, 16h light. Leaf wilting symptoms and the number of dead plants were recorded over time. For *in vitro* infection we used the method previously described in Lu et al (Lu et al., 2018). Briefly, 6-7 day-old Arabidopsis seedlings grown on MS plates were inoculated 1cm away from root tip with a droplet of a solution containing $1x10^7$ cfu of *R. solanacearum* GMI1000, then kept into the growth chamber as detailed above. Root structures were photographed at indicated time points with an Olympus SZX16 microscopy and lateral roots were counted at the indicated times. For the cell death assay, seedlings were immersed into 0.1mg/ml propidium iodide solution and observed under an Olympus confocal microscope IX83-FV1200.

Sample Preparations for RNA-seq

The root samples were collected from around 600 infected seedlings at the indicated time point and frozen in liquid nitrogen, then directly sent to Novogene Company (Beijing, China) which performed RNA seq and data analysis (Supplemental method)

ACKNOWLEDGEMENTS

We thank Pedro L. Rodriguez for providing the *112458* and *12458* ABA receptor mutants. We are also grateful for helps offered by Crop Biology Innovation Platform in Agronomy College in NWAF. This study was supported by the National Natural Science Foundation of China (No. 31601703), the Start-up Funds of Northwest A&F University (Z111021601), the Fundamental Research Fund for the Central Universities of China (Z109021706) and External Science and Technology Cooperation Program of Ningxia Academy of Agriculture and Forestry Sciences (DW-X-2018012). We also acknowledge financial support from the Spanish Ministry of Economy and Competitiveness (grants AGL2016-78002-R and SEV-2015-0533) and from the CERCA project of the Catalan Government (Generalitat de Catalunya).

LITERATURE CITED

An, L., Zhou, Z., Sun, L., Yan, A., Xi, W., Yu, N., Cai, W., Chen, X., Yu, H., Schiefelbein, J., and Gan, Y. 2012. A zinc finger protein gene ZFP5 integrates phytohormone signaling to control root hair development in Arabidopsis. The Plant journal : for cell and molecular biology 72:474-490.

Antoni, R., Gonzalez-Guzman, M., Rodriguez, L., Peirats-Llobet, M., Pizzio, G.A., Fernandez, M.A., De Winne, N., De Jaeger, G., Dietrich, D., Bennett, M.J., and Rodriguez, P.L. 2013. PYRABACTIN RESISTANCE1-LIKE8 plays an important role for the regulation of abscisic acid signaling in root. Plant physiology 161:931-941.

Araya, T., Miyamoto, M., Wibowo, J., Suzuki, A., Kojima, S., Tsuchiya, Y.N., Sawa, S., Fukuda, H., von Wiren, N., and Takahashi, H. 2014. CLE-CLAVATA1 peptide-receptor signaling module regulates the expansion of plant root systems in a nitrogen-dependent manner. Proceedings of the National Academy of Sciences of the United States of America 111:2029-2034.

Baumberger, N., Ringli, C., and Keller, B. 2001. The chimeric leucine-rich repeat/extensin cell wall protein LRX1 is required for root hair morphogenesis in Arabidopsis thaliana. Genes & development 15:1128-1139.

Berens, M.L., Berry, H.M., Mine, A., Argueso, C.T., and Tsuda, K. 2017. Evolution of Hormone Signaling Networks in Plant Defense. Annual review of phytopathology 55:401-425.

Bernoux, M., Timmers, T., Jauneau, A., Briere, C., de Wit, P.J., Marco, Y., and Deslandes, L. 2008. RD19, an Arabidopsis cysteine protease required for RRS1-R-mediated resistance, is relocalized to the nucleus by the Ralstonia solanacearum PopP2 effector. The Plant cell 20:2252-2264.

Berrocal-Lobo, M., Molina, A., and Solano, R. 2002. Constitutive expression of ETHYLENE-RESPONSE-FACTOR1 in Arabidopsis confers resistance to several necrotrophic fungi. The Plant journal : for cell and molecular biology 29:23-32.

Bidadi, H., Matsuoka, K., Sage-Ono, K., Fukushima, J., Pitaksaringkarn, W., Asahina, M., Yamaguchi, S., Sawa, S., Fukuda, H., Matsubayashi, Y., Ono, M., and Satoh, S. 2014. CLE6 expression recovers gibberellin deficiency to promote shoot growth in Arabidopsis. The Plant journal : for cell and molecular biology 78:241-252.

Boursiac, Y., Lee, S.M., Romanowsky, S., Blank, R., Sladek, C., Chung, W.S., and Harper, J.F. 2010. Disruption of the vacuolar calcium-ATPases in Arabidopsis results in the activation of a salicylic acid-dependent programmed cell death pathway. Plant physiology 154:1158-1171.

Caarls, L., Elberse, J., Awwanah, M., Ludwig, N.R., de Vries, M., Zeilmaker, T., Van Wees, S.C.M., Schuurink, R.C., and Van den Ackerveken, G. 2017. Arabidopsis JASMONATE-INDUCED OXYGENASES down-regulate plant immunity by hydroxylation and inactivation of the hormone jasmonic acid. Proceedings of the National Academy of Sciences of the United States of America 114:6388-6393.

Cao, F.Y., Yoshioka, K., and Desveaux, D. 2011. The roles of ABA in plant-pathogen interactions. Journal of plant research 124:489-499.

Chen, Z., Agnew, J.L., Cohen, J.D., He, P., Shan, L., Sheen, J., and Kunkel, B.N. 2007. Pseudomonas syringae type III effector AvrRpt2 alters Arabidopsis thaliana auxin physiology. Proceedings of the National Academy of Sciences of the United States of America 104:20131-20136.

Chung, P.J., Park, B.S., Wang, H., Liu, J., Jang, I.C., and Chua, N.H. 2016. Light-Inducible MiR163 Targets PXMT1 Transcripts to Promote Seed Germination and Primary Root Elongation in Arabidopsis. Plant physiology 170:1772-1782.

Coll, N.S., Vercammen, D., Smidler, A., Clover, C., Van Breusegem, F., Dangl, J.L., and Epple, P. 2010.

Arabidopsis type I metacaspases control cell death. Science 330:1393-1397.

Cui, F., Wu, S., Sun, W., Coaker, G., Kunkel, B., He, P., and Shan, L. 2013. The Pseudomonas syringae type III effector AvrRpt2 promotes pathogen virulence via stimulating Arabidopsis auxin/indole acetic acid protein turnover. Plant physiology 162:1018-1029.

Czernic, P., Visser, B., Sun, W., Savoure, A., Deslandes, L., Marco, Y., Van Montagu, M., and Verbruggen, N. 1999. Characterization of an Arabidopsis thaliana receptor-like protein kinase gene activated by oxidative stress and pathogen attack. The Plant journal : for cell and molecular biology 18:321-327.

De Rybel, B., Vassileva, V., Parizot, B., Demeulenaere, M., Grunewald, W., Audenaert, D., Van Campenhout, J., Overvoorde, P., Jansen, L., Vanneste, S., Moller, B., Wilson, M., Holman, T., Van Isterdael, G., Brunoud, G., Vuylsteke, M., Vernoux, T., De Veylder, L., Inze, D., Weijers, D., Bennett, M.J., and Beeckman, T. 2010. A novel aux/IAA28 signaling cascade activates GATA23-dependent specification of lateral root founder cell identity. Current biology : CB 20:1697-1706.

de Torres-Zabala, M., Truman, W., Bennett, M.H., Lafforgue, G., Mansfield, J.W., Rodriguez Egea, P., Bogre, L., and Grant, M. 2007. Pseudomonas syringae pv. tomato hijacks the Arabidopsis abscisic acid signalling pathway to cause disease. The EMBO journal 26:1434-1443.

Denance, N., Ranocha, P., Oria, N., Barlet, X., Riviere, M.P., Yadeta, K.A., Hoffmann, L., Perreau, F., Clement, G., Maia-Grondard, A., van den Berg, G.C., Savelli, B., Fournier, S., Aubert, Y., Pelletier, S., Thomma, B.P., Molina, A., Jouanin, L., Marco, Y., and Goffner, D. 2013. Arabidopsis wat1 (walls are thin1)-mediated resistance to the bacterial vascular pathogen, Ralstonia solanacearum, is accompanied by cross-regulation of salicylic acid and tryptophan metabolism. The Plant journal : for cell and molecular biology 73:225-239.

Deslandes, L., Olivier, J., Theulieres, F., Hirsch, J., Feng, D.X., Bittner-Eddy, P., Beynon, J., and Marco, Y. 2002. Resistance to Ralstonia solanacearum in Arabidopsis thaliana is conferred by the recessive RRS1-R gene, a member of a novel family of resistance genes. Proceedings of the National Academy of Sciences of the United States of America 99:2404-2409.

Deslandes, L., Pileur, F., Liaubet, L., Camut, S., Can, C., Williams, K., Holub, E., Beynon, J., Arlat, M., and Marco, Y. 1998. Genetic characterization of RRS1, a recessive locus in Arabidopsis thaliana that confers resistance to the bacterial soilborne pathogen Ralstonia solanacearum. Molecular plant-microbe interactions : MPMI 11:659-667.

Digonnet, C., Martinez, Y., Denance, N., Chasseray, M., Dabos, P., Ranocha, P., Marco, Y., Jauneau, A., and Goffner, D. 2012. Deciphering the route of Ralstonia solanacearum colonization in Arabidopsis thaliana roots during a compatible interaction: focus at the plant cell wall. Planta 236:1419-1431.

Evangelisti, E., Govetto, B., Minet-Kebdani, N., Kuhn, M.L., Attard, A., Ponchet, M., Panabieres, F., and Gourgues, M. 2013. The Phytophthora parasitica RXLR effector penetration-specific effector 1 favours Arabidopsis thaliana infection by interfering with auxin physiology. The New phytologist 199:476-489.

Feng, D.X., Tasset, C., Hanemian, M., Barlet, X., Hu, J., Tremousaygue, D., Deslandes, L., and Marco, Y. 2012. Biological control of bacterial wilt in Arabidopsis thaliana involves abscissic acid signalling. The New phytologist 194:1035-1045.

Field, B., and Osbourn, A.E. 2008. Metabolic diversification--independent assembly of operon-like gene clusters in different plants. Science 320:543-547.

French, E., Kim, B.S., Rivera-Zuluaga, K., and Iyer-Pascuzzi, A.S. 2018. Whole Root Transcriptomic Analysis Suggests a Role for Auxin Pathways in Resistance to Ralstonia solanacearum in Tomato. Molecular plant-microbe interactions : MPMI 31:432-444.

Fujii, H., Chinnusamy, V., Rodrigues, A., Rubio, S., Antoni, R., Park, S.Y., Cutler, S.R., Sheen, J., Rodriguez, P.L., and Zhu, J.K. 2009. In vitro reconstitution of an abscisic acid signalling pathway. Nature 462:660-664.

Fujita, Y., Fujita, M., Satoh, R., Maruyama, K., Parvez, M.M., Seki, M., Hiratsu, K., Ohme-Takagi, M., Shinozaki, K., and Yamaguchi-Shinozaki, K. 2005. AREB1 is a transcription activator of novel ABRE-dependent ABA signaling that enhances drought stress tolerance in Arabidopsis. The Plant cell 17:3470-3488.

Genin, S., and Denny, T.P. 2012. Pathogenomics of the Ralstonia solanacearum species complex. Annual review of phytopathology 50:67-89.

Gidda, S.K., Miersch, O., Levitin, A., Schmidt, J., Wasternack, C., and Varin, L. 2003. Biochemical and molecular characterization of a hydroxyjasmonate sulfotransferase from Arabidopsis thaliana. The Journal of biological chemistry 278:17895-17900.

Gimenez-Ibanez, S., Boter, M., Fernandez-Barbero, G., Chini, A., Rathjen, J.P., and Solano, R. 2014. The bacterial effector HopX1 targets JAZ transcriptional repressors to activate jasmonate signaling and promote infection in Arabidopsis. PLoS biology 12:e1001792.

Glazebrook, J. 2005. Contrasting mechanisms of defense against biotrophic and necrotrophic pathogens. Annual review of phytopathology 43:205-227.

Glickmann, E., Gardan, L., Jacquet, S., Hussain, S., Elasri, M., Petit, A., and Dessaux, Y. 1998. Auxin production is a common feature of most pathovars of Pseudomonas syringae. Molecular plant-microbe interactions : MPMI 11:156-162.

Goel, A.K., Lundberg, D., Torres, M.A., Matthews, R., Akimoto-Tomiyama, C., Farmer, L., Dangl, J.L., and Grant, S.R. 2008. The Pseudomonas syringae type III effector HopAM1 enhances virulence on water-stressed plants. Molecular plant-microbe interactions : MPMI 21:361-370.

Gonzalez-Guzman, M., Pizzio, G.A., Antoni, R., Vera-Sirera, F., Merilo, E., Bassel, G.W., Fernandez, M.A., Holdsworth, M.J., Perez-Amador, M.A., Kollist, H., and Rodriguez, P.L. 2012. Arabidopsis PYR/PYL/RCAR receptors play a major role in quantitative regulation of stomatal aperture and transcriptional response to abscisic acid. The Plant cell 24:2483-2496.

Heath, M.C. 2000. Hypersensitive response-related death. Plant molecular biology 44:321-334.

Hernandez-Blanco, C., Feng, D.X., Hu, J., Sanchez-Vallet, A., Deslandes, L., Llorente, F., Berrocal-Lobo, M., Keller, H., Barlet, X., Sanchez-Rodriguez, C., Anderson, L.K., Somerville, S., Marco, Y., and Molina, A. 2007. Impairment of cellulose synthases required for Arabidopsis secondary cell wall formation enhances disease resistance. The Plant cell 19:890-903.

Hirsch, J., Deslandes, L., Feng, D.X., Balague, C., and Marco, Y. 2002. Delayed Symptom Development in ein2-1, an Arabidopsis Ethylene-Insensitive Mutant, in Response to Bacterial Wilt Caused by Ralstonia solanacearum. Phytopathology 92:1142-1148.

Hu, J., Barlet, X., Deslandes, L., Hirsch, J., Feng, D.X., Somssich, I., and Marco, Y. 2008. Transcriptional responses of Arabidopsis thaliana during wilt disease caused by the soil-borne phytopathogenic bacterium, Ralstonia solanacearum. PloS one 3:e2589.

Jiang, C.J., Shimono, M., Sugano, S., Kojima, M., Yazawa, K., Yoshida, R., Inoue, H., Hayashi, N., Sakakibara, H., and Takatsuji, H. 2010. Abscisic acid interacts antagonistically with salicylic acid signaling pathway in rice-Magnaporthe grisea interaction. Molecular plant-microbe

interactions : MPMI 23:791-798.

Jiang, S., Yao, J., Ma, K.W., Zhou, H., Song, J., He, S.Y., and Ma, W. 2013. Bacterial effector activates jasmonate signaling by directly targeting JAZ transcriptional repressors. PLoS pathogens 9:e1003715.

Jiang, Y., Liang, G., Yang, S., and Yu, D. 2014. Arabidopsis WRKY57 functions as a node of convergence for jasmonic acid- and auxin-mediated signaling in jasmonic acid-induced leaf senescence. The Plant cell 26:230-245.

Jones, J.D., and Dangl, J.L. 2006. The plant immune system. Nature 444:323-329.

Kazan, K., and Lyons, R. 2014. Intervention of Phytohormone Pathways by Pathogen Effectors. The Plant cell 26:2285-2309.

Kloek, A.P., Verbsky, M.L., Sharma, S.B., Schoelz, J.E., Vogel, J., Klessig, D.F., and Kunkel, B.N. 2001. Resistance to Pseudomonas syringae conferred by an Arabidopsis thaliana coronatine-insensitive (coi1) mutation occurs through two distinct mechanisms. The Plant journal : for cell and molecular biology 26:509-522.

Lally, D., Ingmire, P., Tong, H.Y., and He, Z.H. 2001. Antisense expression of a cell wall-associated protein kinase, WAK4, inhibits cell elongation and alters morphology. The Plant cell 13:1317-1331.

Le Fevre, R., Evangelisti, E., Rey, T., and Schornack, S. 2015. Modulation of host cell biology by plant pathogenic microbes. Annual review of cell and developmental biology 31:201-229.

Le Roux, C., Huet, G., Jauneau, A., Camborde, L., Tremousaygue, D., Kraut, A., Zhou, B., Levaillant, M., Adachi, H., Yoshioka, H., Raffaele, S., Berthome, R., Coute, Y., Parker, J.E., and Deslandes, L. 2015. A receptor pair with an integrated decoy converts pathogen disabling of transcription factors to immunity. Cell 161:1074-1088.

Lee, D.S., Kim, B.K., Kwon, S.J., Jin, H.C., and Park, O.K. 2009. Arabidopsis GDSL lipase 2 plays a role in pathogen defense via negative regulation of auxin signaling. Biochemical and biophysical research communications 379:1038-1042.

Lee, H.W., and Kim, J. 2013. EXPANSINA17 up-regulated by LBD18/ASL20 promotes lateral root formation during the auxin response. Plant & cell physiology 54:1600-1611.

Lewis, J.D., Wu, R., Guttman, D.S., and Desveaux, D. 2010. Allele-specific virulence attenuation of the Pseudomonas syringae HopZ1a type III effector via the Arabidopsis ZAR1 resistance protein. PLoS genetics 6:e1000894.

Lewis, J.D., Lee, A.H., Hassan, J.A., Wan, J., Hurley, B., Jhingree, J.R., Wang, P.W., Lo, T., Youn, J.Y., Guttman, D.S., and Desveaux, D. 2013. The Arabidopsis ZED1 pseudokinase is required for ZAR1-mediated immunity induced by the Pseudomonas syringae type III effector HopZ1a. Proceedings of the National Academy of Sciences of the United States of America 110:18722-18727.

Li, C., Schilmiller, A.L., Liu, G., Lee, G.I., Jayanty, S., Sageman, C., Vrebalov, J., Giovannoni, J.J., Yagi, K., Kobayashi, Y., and Howe, G.A. 2005. Role of beta-oxidation in jasmonate biosynthesis and systemic wound signaling in tomato. The Plant cell 17:971-986.

Lin, C., Choi, H.S., and Cho, H.T. 2011. Root hair-specific EXPANSIN A7 is required for root hair elongation in Arabidopsis. Molecules and cells 31:393-397.

Lu, H., Lema, A.S., Planas-Marques, M., Alonso-Diaz, A., Valls, M., and Coll, N.S. 2018. Type III Secretion-Dependent and -Independent Phenotypes Caused by Ralstonia solanacearum in Arabidopsis Roots. Molecular plant-microbe interactions : MPMI 31:175-184.

Ma, K.W., and Ma, W. 2016. Phytohormone pathways as targets of pathogens to facilitate infection. Plant molecular biology 91:713-725.

Mansfield, J., Genin, S., Magori, S., Citovsky, V., Sriariyanum, M., Ronald, P., Dow, M., Verdier, V., Beer, S.V., Machado, M.A., Toth, I., Salmond, G., and Foster, G.D. 2012. Top 10 plant pathogenic bacteria in molecular plant pathology. Molecular plant pathology 13:614-629.

Manulis, S., Shafrir, H., Epstein, E., Lichter, A., and Barash, I. 1994. Biosynthesis of indole-3-acetic acid via the indole-3-acetamide pathway in Streptomyces spp. Microbiology 140 (Pt 5):1045-1050.

Melotto, M., Underwood, W., Koczan, J., Nomura, K., and He, S.Y. 2006. Plant stomata function in innate immunity against bacterial invasion. Cell 126:969-980.

Meng, L., and Feldman, L.J. 2010. CLE14/CLE20 peptides may interact with CLAVATA2/CORYNE receptor-like kinases to irreversibly inhibit cell division in the root meristem of Arabidopsis. Planta 232:1061-1074.

Millet, Y.A., Danna, C.H., Clay, N.K., Songnuan, W., Simon, M.D., Werck-Reichhart, D., and Ausubel, F.M. 2010. Innate immune responses activated in Arabidopsis roots by microbe-associated molecular patterns. The Plant cell 22:973-990.

Mitchum, M.G., Yamaguchi, S., Hanada, A., Kuwahara, A., Yoshioka, Y., Kato, T., Tabata, S., Kamiya, Y., and Sun, T.P. 2006. Distinct and overlapping roles of two gibberellin 3-oxidases in Arabidopsis development. The Plant journal : for cell and molecular biology 45:804-818.

Mukhtar, M.S., Deslandes, L., Auriac, M.C., Marco, Y., and Somssich, I.E. 2008. The Arabidopsis transcription factor WRKY27 influences wilt disease symptom development caused by Ralstonia solanacearum. The Plant journal : for cell and molecular biology 56:935-947.

Nahar, K., Kyndt, T., Nzogela, Y.B., and Gheysen, G. 2012. Abscisic acid interacts antagonistically with classical defense pathways in rice-migratory nematode interaction. The New phytologist 196:901-913.

Nomura, K., Debroy, S., Lee, Y.H., Pumplin, N., Jones, J., and He, S.Y. 2006. A bacterial virulence protein suppresses host innate immunity to cause plant disease. Science 313:220-223.

Rauf, M., Arif, M., Fisahn, J., Xue, G.P., Balazadeh, S., and Mueller-Roeber, B. 2013. NAC transcription factor speedy hyponastic growth regulates flooding-induced leaf movement in Arabidopsis. The Plant cell 25:4941-4955.

Rentel, M.C., Lecourieux, D., Ouaked, F., Usher, S.L., Petersen, L., Okamoto, H., Knight, H., Peck, S.C., Grierson, C.S., Hirt, H., and Knight, M.R. 2004. OXI1 kinase is necessary for oxidative burst-mediated signalling in Arabidopsis. Nature 427:858-861.

Robert-Seilaniantz, A., Navarro, L., Bari, R., and Jones, J.D. 2007. Pathological hormone imbalances. Current opinion in plant biology 10:372-379.

Rosquete, M.R., Barbez, E., and Kleine-Vehn, J. 2012. Cellular auxin homeostasis: gatekeeping is housekeeping. Molecular plant 5:772-786.

Sacco, M.A., Koropacka, K., Grenier, E., Jaubert, M.J., Blanchard, A., Goverse, A., Smant, G., and Moffett, P. 2009. The cyst nematode SPRYSEC protein RBP-1 elicits Gpa2- and RanGAP2-dependent plant cell death. PLoS pathogens 5:e1000564.

Saito, S., Hirai, N., Matsumoto, C., Ohigashi, H., Ohta, D., Sakata, K., and Mizutani, M. 2004. Arabidopsis CYP707As encode (+)-abscisic acid 8'-hydroxylase, a key enzyme in the oxidative catabolism of abscisic acid. Plant physiology 134:1439-1449.

Sarris, P.F., Duxbury, Z., Huh, S.U., Ma, Y., Segonzac, C., Sklenar, J., Derbyshire, P., Cevik, V., Rallapalli, G.,

Saucet, S.B., Wirthmueller, L., Menke, F.L.H., Sohn, K.H., and Jones, J.D.G. 2015. A Plant Immune Receptor Detects Pathogen Effectors that Target WRKY Transcription Factors. Cell 161:1089-1100.

Schoenaers, S., Balcerowicz, D., Breen, G., Hill, K., Zdanio, M., Mouille, G., Holman, T.J., Oh, J., Wilson, M.H., Nikonorova, N., Vu, L.D., De Smet, I., Swarup, R., De Vos, W.H., Pintelon, I., Adriaensen, D., Grierson, C., Bennett, M.J., and Vissenberg, K. 2018. The Auxin-Regulated CrRLK1L Kinase ERULUS Controls Cell Wall Composition during Root Hair Tip Growth. Current biology : CB 28:722-732 e726.

Svistoonoff, S., Creff, A., Reymond, M., Sigoillot-Claude, C., Ricaud, L., Blanchet, A., Nussaume, L., and Desnos, T. 2007. Root tip contact with low-phosphate media reprograms plant root architecture. Nature genetics 39:792-796.

Tanaka, H., Kitakura, S., Rakusova, H., Uemura, T., Feraru, M.I., De Rycke, R., Robert, S., Kakimoto, T., and Friml, J. 2013. Cell polarity and patterning by PIN trafficking through early endosomal compartments in Arabidopsis thaliana. PLoS genetics 9:e1003540.

Trujillo, M., Ichimura, K., Casais, C., and Shirasu, K. 2008. Negative regulation of PAMP-triggered immunity by an E3 ubiquitin ligase triplet in Arabidopsis. Current biology : CB 18:1396-1401.

Umezawa, T., Sugiyama, N., Mizoguchi, M., Hayashi, S., Myouga, F., Yamaguchi-Shinozaki, K., Ishihama, Y., Hirayama, T., and Shinozaki, K. 2009. Type 2C protein phosphatases directly regulate abscisic acid-activated protein kinases in Arabidopsis. Proceedings of the National Academy of Sciences of the United States of America 106:17588-17593.

Valls, M., Genin, S., and Boucher, C. 2006. Integrated regulation of the type III secretion system and other virulence determinants in Ralstonia solanacearum. PLoS pathogens 2:e82.

Vasse, J., Genin, S., Frey, P., Boucher, C., and Brito, B. 2000. The hrpB and hrpG regulatory genes of Ralstonia solanacearum are required for different stages of the tomato root infection process. Molecular plant-microbe interactions : MPMI 13:259-267.

Verbon, E.H., and Liberman, L.M. 2016. Beneficial Microbes Affect Endogenous Mechanisms Controlling Root Development. Trends in plant science 21:218-229.

Wasternack, C., and Hause, B. 2013. Jasmonates: biosynthesis, perception, signal transduction and action in plant stress response, growth and development. An update to the 2007 review in Annals of Botany. Annals of botany 111:1021-1058.

Weingart, H., and Volksch, B. 1997. Ethylene Production by Pseudomonas syringae Pathovars In Vitro and In Planta. Applied and environmental microbiology 63:156-161.

Weingart, H., Ullrich, H., Geider, K., and Volksch, B. 2001. The Role of Ethylene Production in Virulence of Pseudomonas syringae pvs. glycinea and phaseolicola. Phytopathology 91:511-518.

Woodward, A.W., and Bartel, B. 2005. Auxin: regulation, action, and interaction. Annals of botany 95:707-735.

Xiao, G., Qin, H., Zhou, J., Quan, R., Lu, X., Huang, R., and Zhang, H. 2016. OsERF2 controls rice root growth and hormone responses through tuning expression of key genes involved in hormone signaling and sucrose metabolism. Plant molecular biology 90:293-302.

Xie, Q., Frugis, G., Colgan, D., and Chua, N.H. 2000. Arabidopsis NAC1 transduces auxin signal downstream of TIR1 to promote lateral root development. Genes & development 14:3024-3036.

Zhang, Z., Lenk, A., Andersson, M.X., Gjetting, T., Pedersen, C., Nielsen, M.E., Newman, M.A., Hou, B.H., Somerville, S.C., and Thordal-Christensen, H. 2008. A lesion-mimic syntaxin double mutant in

Arabidopsis reveals novel complexity of pathogen defense signaling. Molecular plant 1:510-527.

Zhao, Y. 2010. Auxin biosynthesis and its role in plant development. Annual review of plant biology 61:49-64.

Zhou, Z., Wu, Y., Yang, Y., Du, M., Zhang, X., Guo, Y., Li, C., and Zhou, J.M. 2015. An Arabidopsis Plasma Membrane Proton ATPase Modulates JA Signaling and Is Exploited by the Pseudomonas syringae Effector Protein AvrB for Stomatal Invasion. The Plant cell 27:2032-2041.

SUPPORTING INFORMATION LEGENDS

Figure S1. GMI1000 promotes lateral root formation. 7-day-old Arabidopsis seedling roots were inoculated with GMI1000 suspension or water. Lateral roots were counted and recorded at 5 dpi.

Figure S2. Selected GO term overrepresented in differentially expressed genes at different infection stages of GMI1000. GO terms in upper boxes indicate up-regulated genes and GO terms in lower boxes indicate down-regulated genes.

Figure S3. Biosynthesis and signaling components of ET and JA during the early stages of GMI1000 infection. (A) Heat map representation of differentially expressed genes in ET biosynthesis and signaling pathways. (B) Heat map representation of differentially expressed genes involved in JA biosynthesis and signaling pathways. The heat map depicts FPKM values after log10 transformation.

Figure S4. Activation of auxin pathway in response to GMI1000 infection. Heat map values represent $\log_{10}$-transformed FPKM values.

Figure S5. Transcriptional changes of part of differentially expressed genes involved in plant immunity. Heat map values represent $\log_{10}$-transformed FPKM values.

Table S1. Overview of quality of RNA-seq data.

Data S1. FPKM values of 2698 differentially expressed genes in root at each time points after GMI1000 treatment

Data S2. Membership of 11 gene clusters.

Data S3. Summary of all of differentially expressed genes which play key roles

in plant immunity.

FIGURE LEGENDS

Figure 1. Time series of root structure after GMI1000 infection. (A) Root growth was recorded and digital images were taken images at indicated time points. The arrow indicates lateral roots. Dashed line indicates root growth arrest. (B) Root hair images were taken with an OLYMPUS SZX16 microscope at the indicated time points. (C) Cell death on the root tip was stained with a PI solution and images were directly taken with an Olympus confocal microscope.

Figure 2. Clustering analysis of RNAseq data. The heat map represents the expression patterns of 2698 DEGs identified in our RNA-seq data. The vertical axis organizes genes according to co-expression patterns. The horizontal axis displays time points. Red represents genes with high expression while blue represents genes with low expression. The selected overpresented GO terms in each cluster were shown on the left. The heat map depicts FPKM value after $\log_{10}$ transformation. .

Figure 3. Expression patterns of part of genes related with auxin biosynthesis, signaling and transport. (A) Auxin biosynthesis processes and metabolic processes. Differentially expressed enzymes in our RNA-seq data are shown in black bold, otherwise enzymes are shown in gray bold. (B) Expression patterns of differentially expressed auxin biosynthetic genes in response to GMI1000 infection. (C) Expression patterns of differentially expressed auxin signaling components in response to GMI1000. (D) Expression patterns of differentially expressed auxin transport in response to GMI1000. The heat map depicts FPKM values after $\log_{10}$ transformation.

Figure 4. ABA receptor mutants *12458* and *112458* showed more sensitivity to GMI1000. (A) Temporal dynamics of ABA signal components after GMI1000 treatment. Heat map depicts the expression patterns of differentially expressed ABA-responsive genes. (B) Wilt symptoms weredigitally imaged at 15 dpi. (C) Mortality rate of the infected plants was recorded at indicated times. **

indicates P<0.001 (Student's test) with respect to Col-0.

Figure 5. Mutations in ABA receptors did not abolish root architecture changes caused by GMI1000. (A) Inhibition of *112458* root growth. Primary root elongation length after infection was measured at 4 dpi. (B) Root hair formation on *112458* root tips. The images were taken with Olympus microscope. (C) Lateral roots on *112458* root. Lateral roots per seedling were counted and recorded at 4 dpi

Figure 6. Expression dynamics of components of programmed cell death over the infection time. (A) Heat map depicting differentially expressed genes in effector –triggered hypersensitive responses. (B) Heat map representation of differentially expressed components of senescence. Heat map values represent log_{10}-transformed FPKM values.

Figure 7. Expression of genes regulating root hair formation correlated with root hair formation. (A) Heat map representation of differentially expressed genes in root hair formation after GMI1000 infection. Heat map values represent log_{10}-transformed FPKM values. (B) Root hair appeared at 18h after GMI1000 infection. The pictures were taken with an Olympus microscope at the indicated time after infection.

Figure 8. Transcriptional dynamic changes of differentially expressed genes in root architecture. Heat map values represent log_{10}-transformed FPKM values.

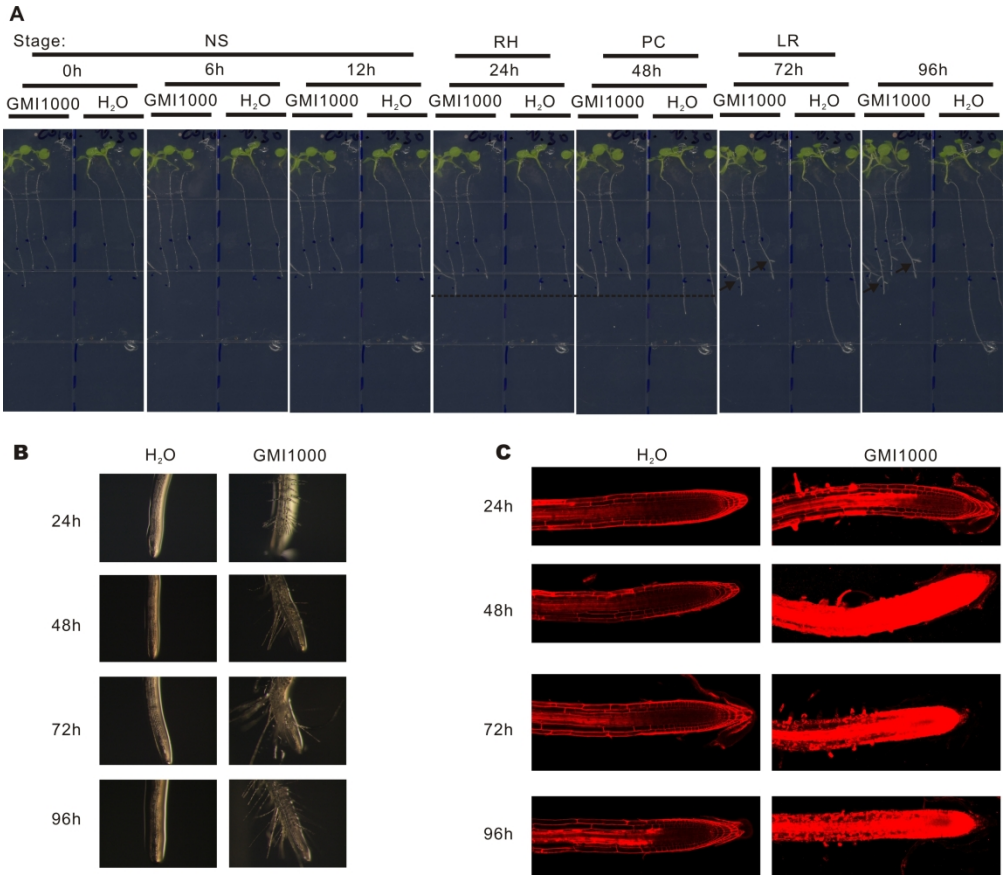

Time series of root structure after GMI1000 infection

148x128mm (600 x 600 DPI)

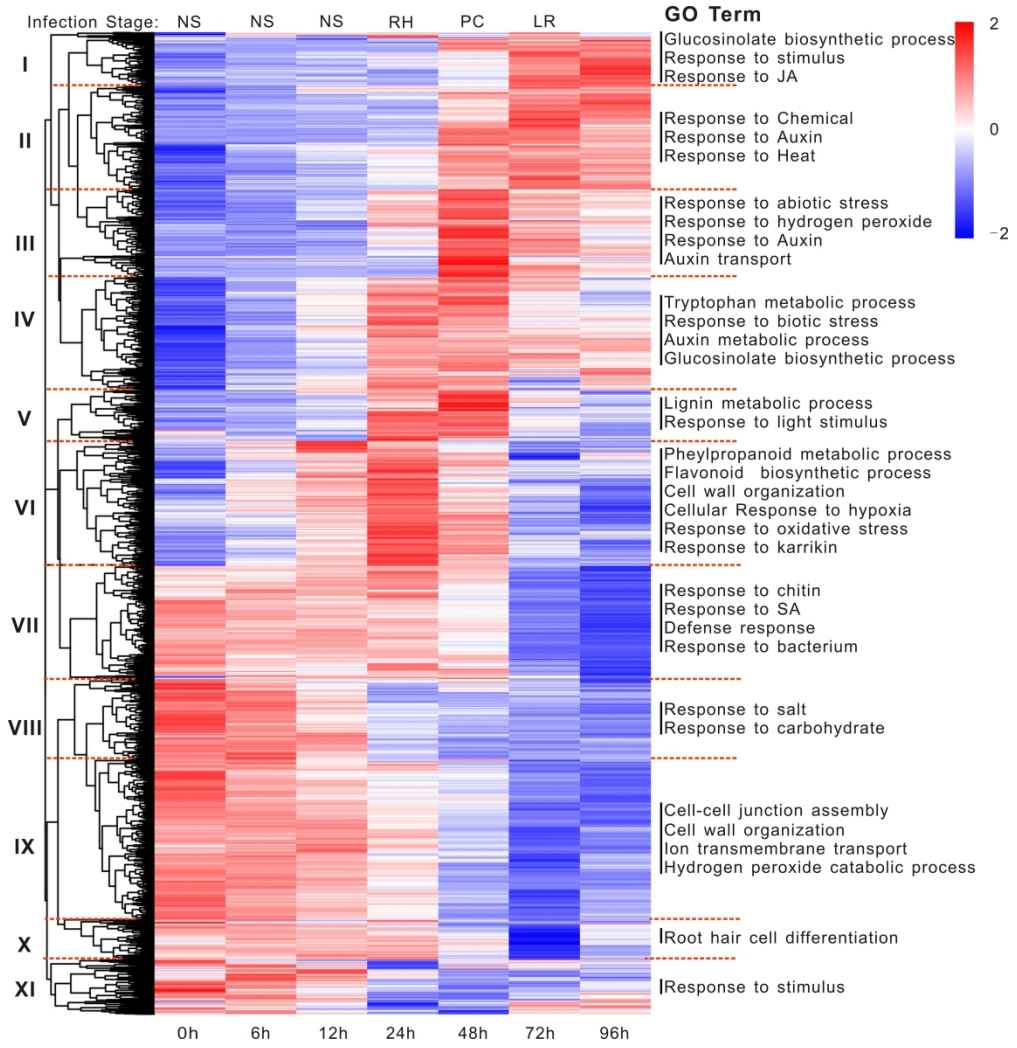

Clustering analysis of RNAseq data

174x179mm (600 x 600 DPI)

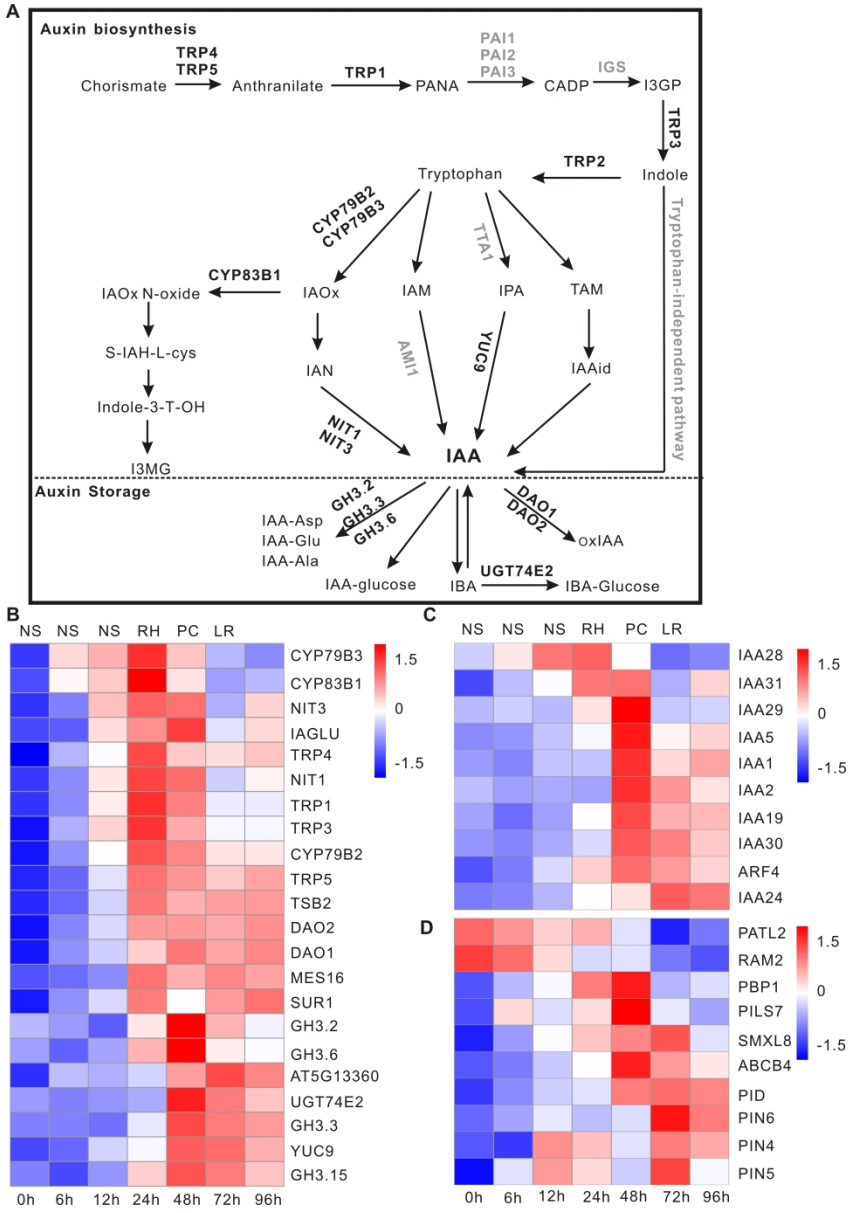

Expression patterns of part of genes related with auxin biosynthesis, signaling and transport

221x315mm (600 x 600 DPI)

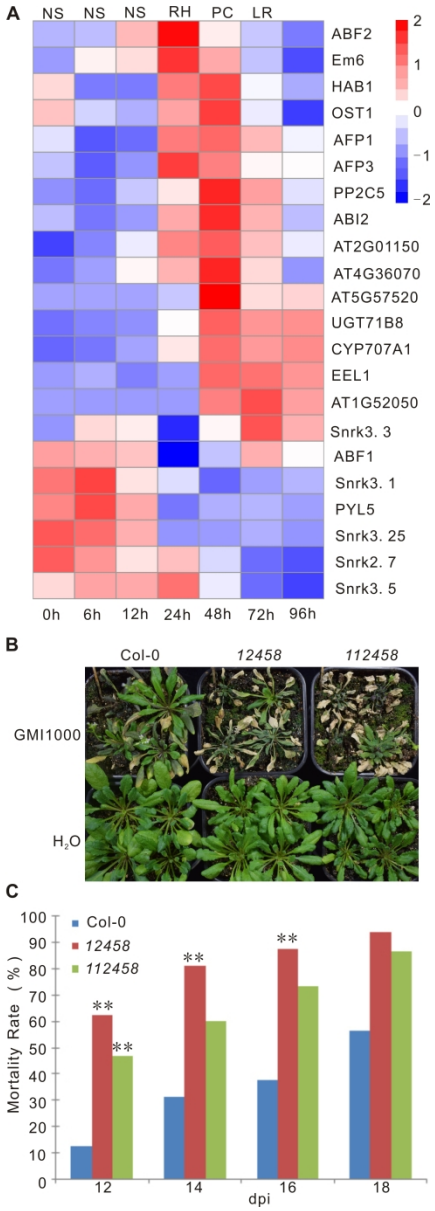

ABA receptor mutants 12458 and 112458 showed more sensitivity to GMI1000

223x624mm (600 x 600 DPI)

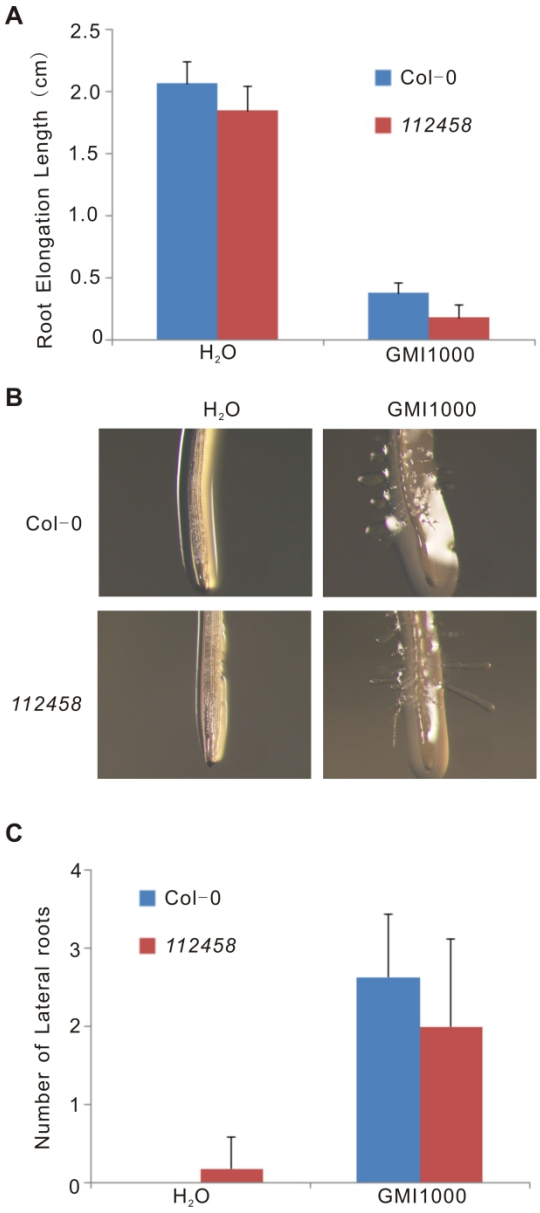

Mutations in ABA receptors did not abolish root architecture changes caused by GMI1000

168x377mm (600 x 600 DPI)

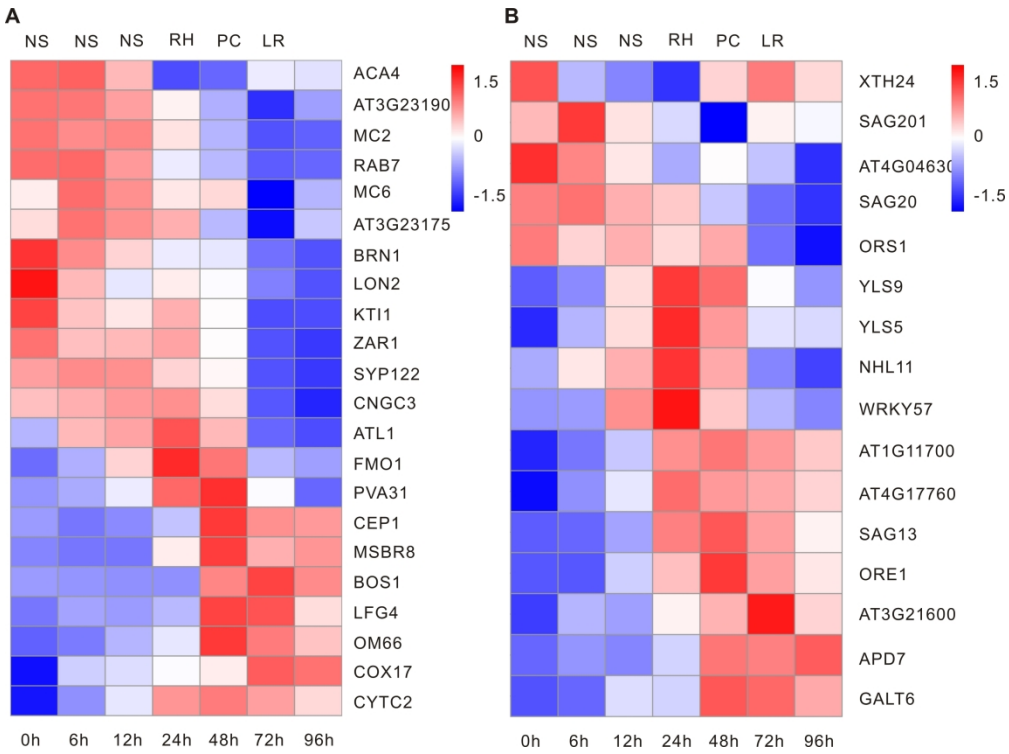

Expression dynamics of components of programmed cell death over the infection time

123x91mm (600 x 600 DPI)

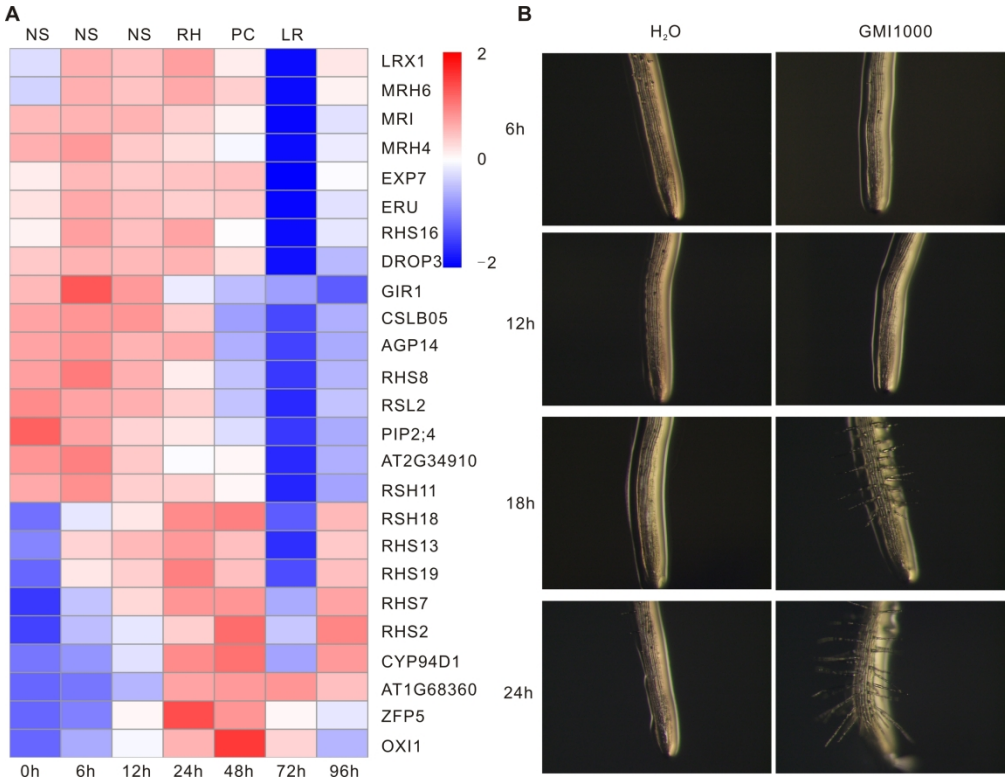

Expression of genes regulating root hair formation correlated with root hair formation

130x100mm (600 x 600 DPI)

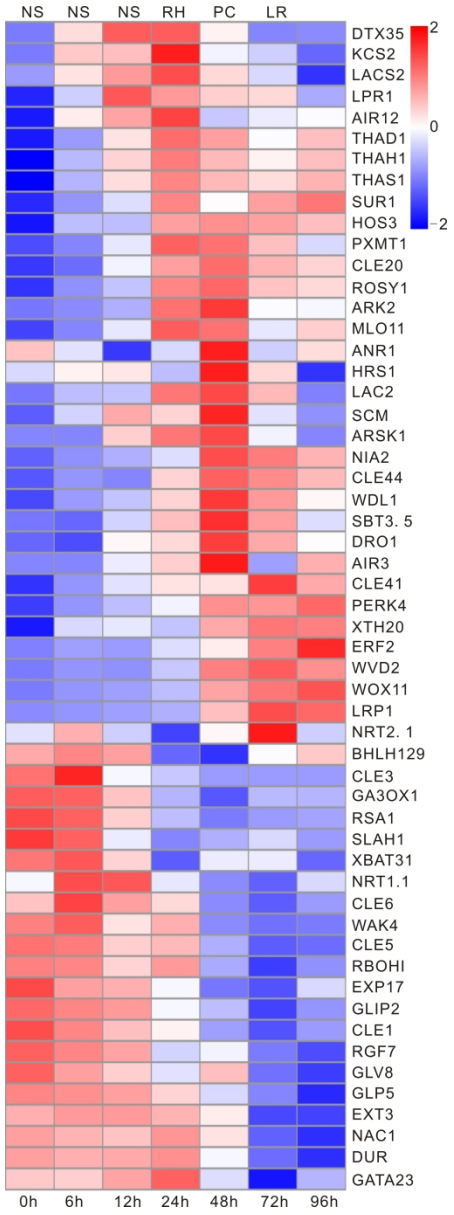

Transcriptional dynamic changes of differentially expressed genes in root architecture

216x586mm (600 x 600 DPI)

SUPPLEMENTAL DATA

Deep sequencing reveals that early reprogramming of Arabidopsis root transcriptomes upon *Ralstonia solanacearum* infection

Overview

Supplemental Methods

Supplemental References

Supplemental Tables: Table S1

Supplemental Methods

Sample Preparations for RNA-seq

The root samples were collected from around 600 infected seedlings at the indicated time point and fronzen in liquid nitrogen, then directly sent to Novogene Company (Beijing, China) and perform RNA seq and data analysis there.

RNA Extraction, Library Preparation and Sequencing (Novogene)

RNA were extracted using Trizol. After RNA extraction, RNA quality and quantitiy were assessed with following equipments: Nano Photometer spectrophotometer (IMPLEN,CA, USA) for RNA purity, Qubit®RNA Assay Kit in Qubit® 2.0 Flurometer (Life Technologies, CA, USA) for RNA concentration, RNA Nano 6000 Assay Kit of the Bioanalyzer 2100 system (Agilent Technologies, CA, USA) for RNA integrity.

A total amount of 3 μg RNA per sample was used as input material for the RNA sample preparations. Sequencing libraries were generated using NEBNext® Ultra™ RNA Library Prep Kit for Illumina® (NEB, USA) following manufacturer's recommendations and index codes were added to attribute sequences to each sample. Briefly, mRNA was purified from total RNA using poly-T oligo-attached magnetic beads. Fragmentation was carried out using divalent cations under elevated temperature in NEB Next First Strand Synthesis Reaction Buffer (5X). First strand cDNA was synthesized using random hexamer primer and M-MuLV Reverse Transcriptase (RNaseH). Second strand cDNA synthesis was subsequently performed using DNA Polymerase I and RNase H. Remaining overhangs were converted into blunt ends via exonuclease/polymerase activities. After adenylation of 3' ends of DNA fragments, NEB Next Adaptor with hairpin loop structure were ligated to prepare for hybridization. In order to select cDNA fragments of preferentially 150~200 bp in length, the library fragments were purified with AMPure XP system (Beckman Coulter, Beverly, USA). Then 3 μl USER Enzyme (NEB, USA) was used with size-selected, adaptor-ligated cDNA at 37°C for 15 min followed by 5 min at 95 °C before PCR. Then PCR was performed with

Phusion High-Fidelity DNA polymerase, Universal PCR primers and Index (X) Primer. At last, PCR products were purified (AMPure XP system) and library quality was assessed on the Agilent Bioanalyzer 2100 system

The clustering of the index-coded samples was performed on a cBot Cluster Generation System using TruSeq PE Cluster Kit v3-cBot-HS (Illumia) according to the manufacturer's instructions. After cluster generation, the library preparations were sequenced on an Illumina Hiseq platform and 125bp/150 bp paired-end reads were generated.

Data Analysis: Quality Control, Reads Mapping to Genome, Quantification of Gene Expression level and Differential Expression Analysis (Novogene)

Raw data (raw reads) of fastq format were firstly processed through in-house perl scripts. In this step, clean data (clean reads) were obtained by removing reads containing adapter, reads containing ploy-N and low quality reads from raw data. At the same time, Q20, Q30 and GC content of the clean data were calculated. All the downstream analyses were based on the clean data with high quality.

Arabidopsis genome and gene model annotation files were downloaded from Ensemble database Version 34 directly. Index of the reference genome was built using Hisat2 v2.0.4 and paired-end clean reads were aligned to the reference genome using Hisat2 v2.0.4 (Kim et al., 2015). We selected Hisat2 as the mapping tool for that Hisat2 can generate a database of splice junctions based on the gene model annotation file and thus a better mapping result than other non-splice mapping tools.

HTSeq v0.6.1was used to count the reads numbers mapped to each gene (Anders et al., 2015). And then FPKM of each gene was calculated based on the length of the gene and reads count mapped to this gene. FPKM, expected number of Fragments Per Kilobase of transcript sequence per Millions base pairs sequenced, considers the effect of sequencing depth and gene length for

the reads count at the same time, and is currently the most commonly used method for estimating gene expression levels (Trapnell et al., 2010).

Differential expression analysis of two conditions/groups (two biological replicates per condition) was performed using the DESeq R package (1.18.0) (Anders and Huber 2012). DESeq provide statistical routines for determining differential expression in digital gene expression data using a model based on the negative binomial distribution (Anders and Huber, 2010). The resulting P-values were adjusted using the Benjamini and Hochberg's approach for controlling the false discovery rate. Genes with an adjusted P-value <0.05 found by DESeq and fold change (-1>log2>1) were assigned as differentially expressed.

Clustering of Gene Expression Profiles (Novogene)

Cluster analysis is used to determine the expression patterns of differential genes under different experimental conditions. Heatmap represents the expressions of all differentially expressed genes identified in the RNA-seq experiment. The FPKM value of differential genes under different experimental conditions was used as the expression level, and hierarchical clustering analysis was performed. Different colored regions represent different clustering grouping information. The X-axis represents sample name and the Y-axis represents the differentially expressed genes. Expression data was normalized in log10 (FPKM+1) manner, heatmaps were drawn by R pheatmap package (Kolde, 2018).

GO Analysis

GO annotation analysis was performed using the Agrigo v2.0 (Tian *et al.*, 2017). Overrepresented GO_Biological_Process categories were identified using a hypergeometric test with FDR<0.05 with the whole annotated genome as the reference test.

Supplemental References

Anders, S. and Huber, W. (2010) Differential expression analysis for sequence count data. *Genome biology*, **11**, R106.

Anders S, Huber W (2012) Differential expression of RNA-seq data at the gene level- the DESeq package

Anders, S., Pyl, P.T. and Huber, W. (2015) HTSeq--a Python framework to work with high-throughput sequencing data. *Bioinformatics*, **31**, 166-169.

Kim, D., Langmead, B. and Salzberg, S.L. (2015) HISAT: a fast spliced aligner with low memory requirements. *Nature methods*, **12**, 357-360.

Klode, R.(2018) Pretty Heatmaps Package 'pheatmap' version 1.0.10

Tian T, Liu Y, Yan H, You Q, Yi X, Du Z, Xu W, Su Z. 2017. agriGO v2.0: a GO analysis toolkit for the agricultural community, 2017 update. Nucleic Acids Res **45**, W122-W129.

Trapnell, C., Williams, B.A., Pertea, G., Mortazavi, A., Kwan, G., van Baren, M.J., Salzberg, S.L., Wold, B.J. and Pachter, L. (2010) Transcript assembly and quantification by RNA-Seq reveals unannotated transcripts and isoform switching during cell differentiation. *Nature biotechnology*, **28**, 511-515.

Supplemental Tables

Supplemental Table S1. Overview of quality of RNA-seq data.

Sample name	Raw reads	Clean reads	Clean bases (Gb)	Mapped reads (% of total)	Q30(%)
G0	34305303	33278781	4.99	31560849 (94.86%)	91.37
G6	36097955	34998502	5.25	33069200 (94.50%)	92.30
G12	39001013	37994586	5.70	36226397 (95.38%)	91.40
G24	34175878	33150365	4.97	31537042 (95.16%)	91.74
G48	33370411	32175593	4.82	30628497 (95.19%)	91.78
G72	32732665	31887137	4.78	30067895 (94.51%)	91.44
G96	35598467	34544686	5.18	32460784 (94.07%)	92.06
H96	35542801	34630479	5.19	32848338 (94.89%)	91.74

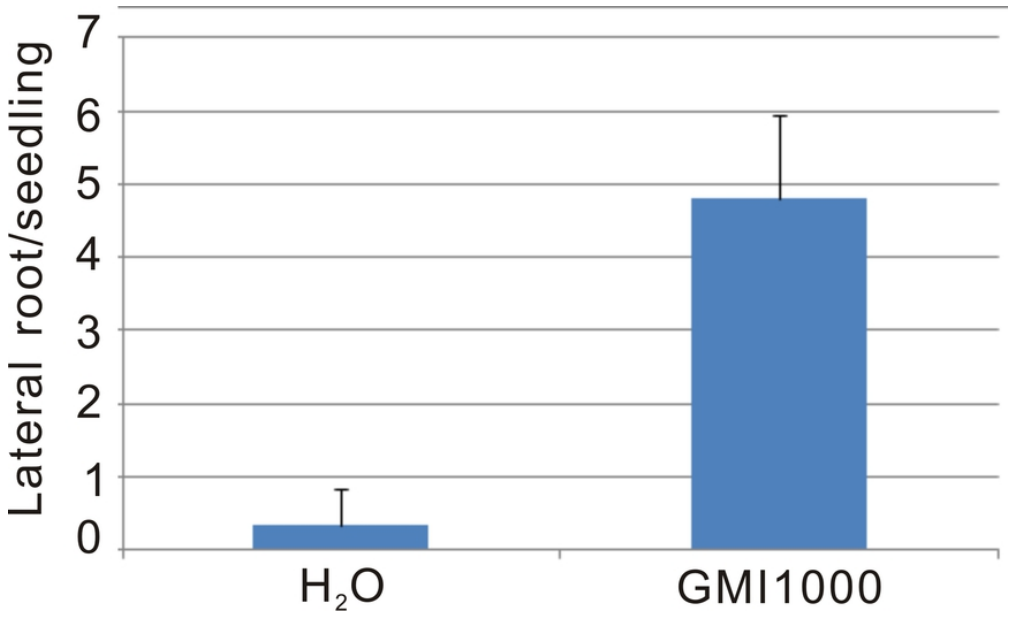

GMI1000 promotes lateral root formation

36x22mm (600 x 600 DPI)

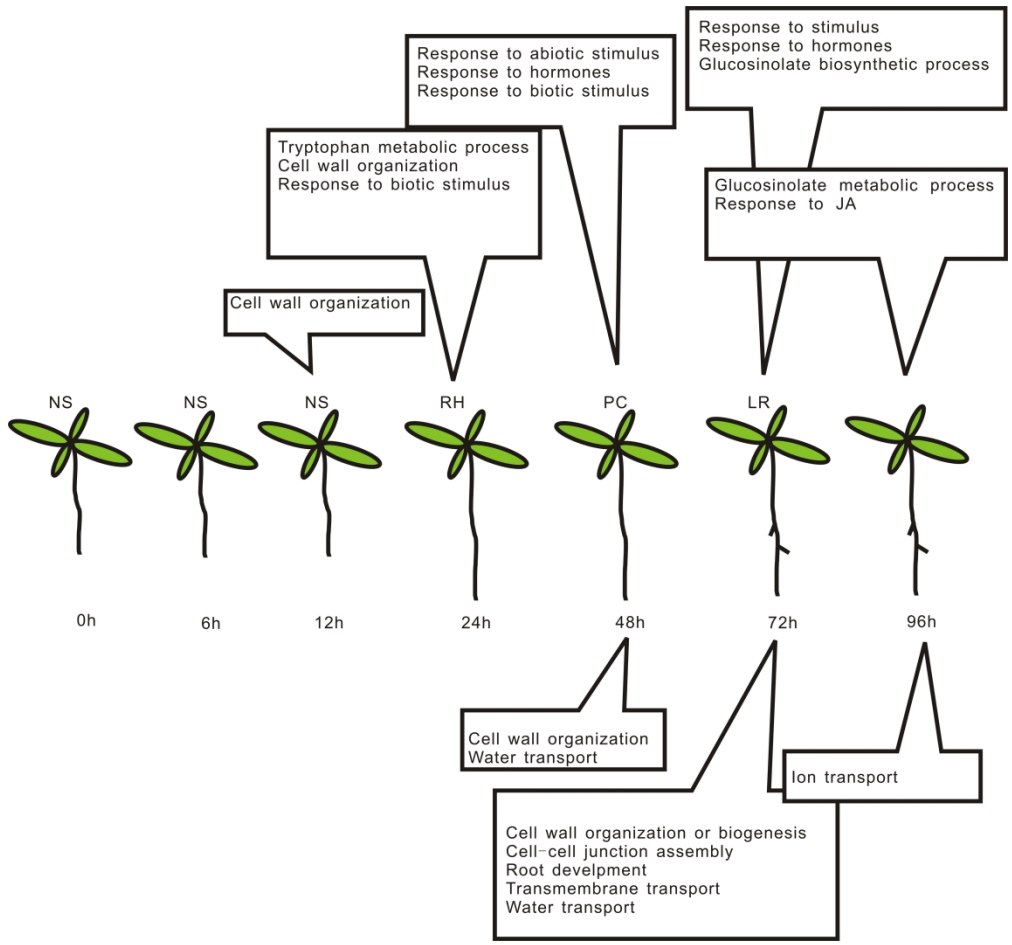

Selected GO term overrepresented in differentially expressed genes at different infection stages of GMI1000

158x147mm (600 x 600 DPI)

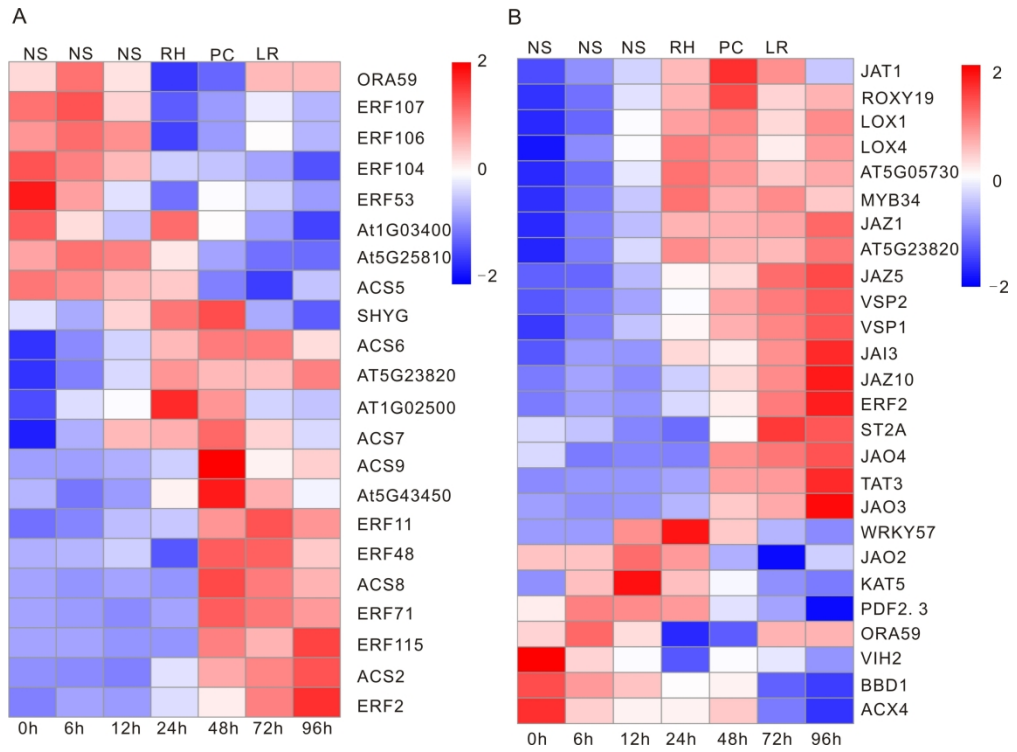

Selected GO term overrepresented in differentially expressed genes at different infection stages of GMI1000

121x89mm (600 x 600 DPI)

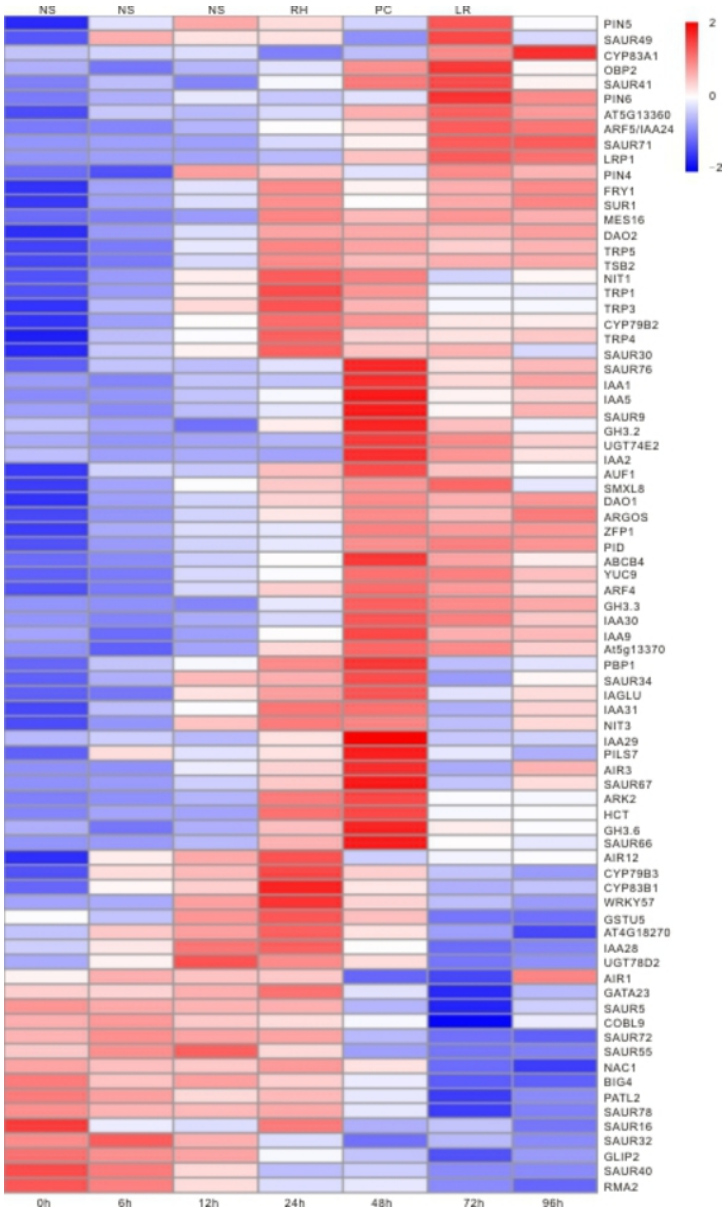

Activation of auxin pathway in response to GMI1000 infection

23x40mm (600 x 600 DPI)

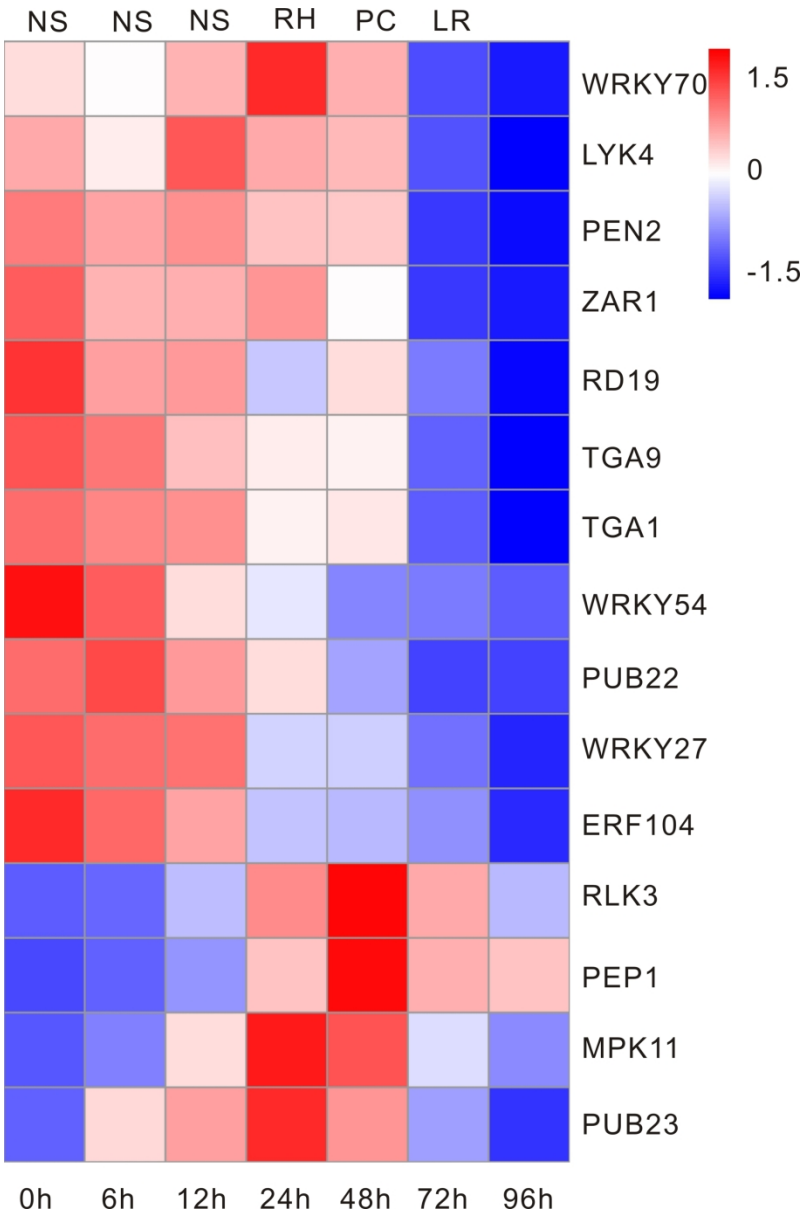

Transcriptional changes of part of differentially expressed genes involved in plant immunity.

117x177mm (600 x 600 DPI)